# Effect of Series Active Voltage Conditioners on Modernized Grid

*A thesis*

*submitted in fulfillment*

*of the requirements for the degree of*

*Master of Engineering*

*in*

*Electrical Engineering*

*at*

*Victoria University of Wellington*

*by*

*Mostafa Ahmed Nazih Ahmed*

Victoria
UNIVERSITY OF WELLINGTON
Te Whare Wānanga
o te Ūpoko o te Ika a Māui

www.vuw.ac.nz

**2015**

*To my mother.....a hopeful apology*

# ABSTRACT

Modernized “Smart” grids incorporate renewable energy sources on a widespread scale. Foreseen expansion in integrating more renewables is driven by global $CO_2$ emission concerns and depletion of fossil fuels. Active elements/devices are added to smart grids to enhance power availability and quality with the aid of advances in power electronics and communication systems. Active Voltage Conditioner (AVC) represents state-of-the-art in the field of voltage regulation and conditioning, however; integrating it into modernized grids has not been the subject of detailed study yet.

This thesis details the AVC-Grid interaction mechanism and associated performance parameters. ABB PCS100 AVC computer model based on MATLAB/PLECS platform is used as a basis for the proposed mathematical model. Accordingly, operational V-I characteristics is derived and impact of equivalent grid stiffness is analyzed.

In this thesis, the modeling of AVC has been introduced as seen by the grid in light of MATLAB/PLECS simulations. The conditioning ratio to describe the “depth” of load conditioning had been introduced. Modeling of AVC operational characteristics has been developed and dependency on conditioning ratio and equivalent grid stiffness had been investigated. Also, the analysis of grid behavior due to AVC operation during overvoltages and undervoltages has been carried out as well as discussing the envisaged impact on tied WTG/PV systems.

The thesis represents an initial attempt to model the AVC and discusses its envisaged impact on smart grids.

# ACKNOWLEDGEMENTS

I would like to get the opportunity to thank everyone who helped and encouraged me to carry out this thesis through both technical and non-technical difficulties I have faced during the last two years.

Dr.Ramesh Rayudu has been very helpful and patient with my progress into the study and his advises and cooperation exceed what words here may reflect. Much obliged to you.

I should not miss Nick Elliot for accepting my request initially to carry out this study with ABB NZ.

Dr.Simon Walton cooperated extensively with me bearing my endless questions and enquiries about AVC. Without his notes and guidance this thesis could never be realized.

Nick E. and Simon W. have welcomed Victoria University of Wellington staff members and me to ABB NZ factory in Napier in 2013.

Many thanks to Dr.Mohamed El-Shimy, Ain Shams University, Cairo, Egypt for his fruitful discussion and guidance he provided.

My immediate family encouraged me to continue my research and paved the way for this progress in my professional and academic life. My gratitude to all of you.

And finally I have to thank my fellow colleagues who helped and supported me into completing this work.

# GLOSSARY OF TERMS & SYMBOLS

| | |
|---|---|
| $\phi$ | Load power angle (rad) |
| $\Delta I_g$ | Additional grid supply current due to AVC operation (p.u.). |
| $\Delta Q_g$ | Additional reactive power demand due to the operation of AVC (p.u.) |
| $\Delta V$ | PCC voltage variation from system nominal (p.u.) |
| $\Delta V_a$ | Additional PCC voltage variation due to additional AVC demand (p.u.) |
| AC | Alternating Current |
| AVC | Active Voltage Conditioner |
| AVQR | Active Voltage Quality Regulator |
| AVR | Automatic Voltage Regulator |
| CPL | Constant Power Load |
| *d*-axis | Direct Axis (machine rotor) |
| DC | Direct Current |
| DFIG | Doubly Fed Induction Generator |
| DG | Distributed Generation |
| DVR | Dynamic Voltage Restorer |
| EMF | Electro Motive Force |
| EMI | Electromagnetic Interference |
| $E_{th}$ | Supply grid Thévinin equivalent EMF (p.u.) |
| HV | High Voltage (voltages greater than 69 kV) |
| HVAC | Heating, Ventilation and Air Conditioning |
| HVRT | High Voltage Ride-Through |
| $I_g$ | Grid supply current (p.u.) |
| $I_n$ | Load nominal current (p.u.) |
| $I_f$ | Short circuit current (p.u.) |
| IEEE | Institute of Electrical and Electronics Engineers |
| KVL | Kirchhoff's Voltage Law |
| LSC | Line Side Converter |
| LV | Low Voltage (voltages up to and including1 kV) |
| LVRT | Low Voltage Ride-Through |
| MPPT | Maximum Power Point Tracking |
| MV | Medium Voltage (ranging from >1 kV to 69 kV) |
| NGR | Neutral Grounding Resistor |
| NZ | New Zealand |

| | |
|---|---|
| OLTC | On-Load Tap Changer |
| O/V | Overvoltage |
| p.u. | Per Unit |
| $P_{AVC}$ , $P_C$ | AVC demand active power (p.u.) |
| PCC | Point of Common Coupling (where AVCs are connected) |
| PF | Power Factor (%, p.u.) |
| PLECS® | Piecewise Linear Electrical Circuit Simulation |
| PLL | Phase Locked Loop |
| PV | Photovoltaic |
| *q*-axis | Quadrature Axis (machine rotor) |
| $Q_{AVC}$, $Q_C$ | AVC demand reactive power (p.u.) |
| $Q_{No\text{-}AVC}$ | Load reactive power in case of no AVC is activated (p.u.) |
| R&D | Research and Development |
| RSC | Rotor Side Converter |
| $S_{AVC}$ | AVC demand apparent power (p.u.) |
| $S_c$ | Total conditioned load (p.u.) |
| $S_g$ | Demand as seen by supply grid on PCC (p.u.) |
| $S_n$ | Load nominal apparent power (p.u.) |
| $S_{sc}$ | Supply grid short circuit capacity (p.u.) |
| $S_t$ | Total PCC load (p.u.) |
| $S_{uc}$ | Total unconditioned load (p.u.) |
| SCR | Short Circuit Ratio |
| SLD | Single Line Diagram |
| SLG | Single Line-to-Ground (fault type) |
| THDv | Total Harmonic Distortion – voltage based. (%) |
| U/V | Undervoltage |
| $V_n$ | System nominal voltage (p.u.) |
| $V_{PCC}$ | AVC input voltage on PCC (p.u.) |
| VA | Volt-Ampere |
| VFD | Variable Frequency Drive |
| WTG | Wind Turbine Generator |
| *x* | Conditioning ratio |
| $Z_c$ | Conditioned load impedance (p.u.) |
| $Z_{uc}$ | Unconditioned load impedance (p.u.) |
| $Z_s$ | Supply grid short circuit impedance (p.u.) |
| $Z_t$ | Total PCC load impedance (p.u.) |

# TABLE OF CONTENTS

# LIST OF FIGURES

# LIST OF TABLES

# 1 Introduction

## 1.1 Background

The world trend in power generation is heading towards integrating more renewable energy sources into *smart grids* in particular. Renewable energy penetration in modernized grids is running around 20-30% with intermittent figures exceeding 50% [1]. Studies for up to 90% penetration are taking place around North America where the need for reliable and secure power is crucial [2]. The higher renewable energy penetration level is associated with stability concerns with more generation intermittency. Accordingly, voltage fluctuations on Point of Common Coupling (PCC) appear with variable power flow.

## 1.2 The Problem of Voltage Fluctuations

Industrial and commercial electricity consumers are mostly concerned with productivity loss due to voltage sags/swells especially with increased use of sensitive electronic and power electronics process control equipment. Millions of dollars are lost every year due to insignificant voltage sags causing production lines to halt as well as networks to mal-operate [3].

Voltage profile within grid is helpful into predicting the ride-through capability of tied renewable energy sources. The need for voltage regulation on sensitive power loads justifies using Active Voltage Conditioners (AVCs) to stabilize the load voltage with minimal deviation (zero, ideally) from nominal voltage over the grid operational voltage range (European standards allow up to ±10% voltage variation from nominal value) [4].

## 1.3 Aim of the Thesis

The study aims to investigate the impact of using Active Voltage Conditioners (AVCs) on integrated renewable energy sources. Investigating the operation of AVC on the grid side voltage will be the key parameter to analyze the envisaged impact on tied renewable energy resources. The thesis describes the AVC performance and determine its parameters and dependencies.

The study highlights the basic performance parameters ascribed to AVC operation like voltage variations, current demand, reactive power demand, load impedance,

power factor, response time, efficiency and harmonic distortion. Unsymmetrical operation should be addressed within the thesis.

## 1.4 Methodology

MATLAB/PLECS model for PCS100 AVC series manufactured by ABB NZ has been used within this thesis to investigate the operational impact on smart/modernized grid with high renewable energy penetration. Simulation output (Chapter 3) is used as a basis for AVC mathematical modeling (Chapter 4). Operational V-I characteristics is derived accordingly.

Operation of AVC is characterized by very fast response (around half a cycle) compared with other voltage regulation techniques e.g. OLTCs (up to 10 minutes) which enables them to act during short time transient voltage abnormalities. Remote system faults, motor starting, load and generation rejection mostly do not last enough to cause AVR/OLTC to respond. Nevertheless, AVCs will respond to such disturbances collectively at the same Point of Common Coupling (PCC), at the same time.

The application of AVCs has not been studied much within the industry, and a possible area for development may exist within modern grids with engineered application of new technologies.

## 1.5 Thesis Outline

The thesis is split into **five** chapters as follows:

**Chapter 1**: This chapter introduces for the need for voltage regulation within grids with high renewable energy penetration and associated voltage fluctuations. Aim of the thesis and its outline are included.

**Chapter 2**: This chapter lists more detailed description for elements of system under study and associated operational abnormalities.

**Chapter 3**: This chapter is dedicated to describe Active Voltage Conditioner (AVC) construction and operation. PLECS/Simulink simulation results are provided.

**Chapter 4**: This chapter lists the investigation carried out to predict the AVC-Grid interaction. Detailed mathematical modeling for AVC is derived and associated V-I characteristics are developed based on PLECS/Simulink

simulation results in Chapter 3. In light of modeling results, envisaged AVC impact on modernized grids is discussed.

**Chapter 5**: This chapter summarizes the study conclusions and lists recommendations for further related research points.

References and bibliography contains a list of citations and reference material and literature at the end of the thesis.

# 2 Literature Review:

## 2.1 Smart Grid

With the widespread use of Distributed Generation (DG) within networks, and the current trend of communication systems, the concept of “smart” gird evolves to compose a real-time controlled grid that achieves reliable and economic operation and interaction between generation and consumers. Voltage regulation within smart grids is of particular importance with various methods of control [5]. The bi-directional power flow among the smart grid raises the challenge of using flexible automatic and distributed voltage regulators working on real-time environment.

The concept of smart grid is very helpful into integrating renewable energy sources due to stochastic intermittency nature of generated power. With the growing high penetration of renewable energy sources, the smart grid proves to be deemed necessary in order to achieve system reliability, stability and dispatchability.

Load flow among various elements of the grid with distributed generation can result in unpredictable voltage profiles. Accordingly, the need for fast and reliable voltage conditioning arises. Since the aggregation of sources and loads is possible with the virtue of linear operators, the thesis will focus on analyzing voltages at Point of Common Coupling (PCC) with connected AVCs, conventional generation and renewable energy source.

## 2.2 Renewable Energy Sources

Major generated power contribution from renewable energy sources-excluding hydro-comes from wind turbine generators (WTG) and photovoltaic cells (PV). Allocation of renewable energy sources is decided based on historical records of the availability of wind and solar insolation for economic feasibility of the installations.

### 2.2.1 Wind Turbine Generators (WTG)

Growth of wind power around the world is exceeding the optimistic expectations of the past years [6]. 20-30% installed capacity penetration of wind power generation cannot be missed within Italy, Denmark & Germany. Intermitting penetration may rise to about 50% [1].

Horizontal axis wind turbines are typically used both onshore and offshore for utility scale generation. Rotor diameters may exceed 100 m (offshore) with supporting masts supporting them for “free from turbulences” wind. Figure 2-1 shows typical horizontal axis wind turbine construction. An upstream wind turbine rotor is oriented into the prevailing wind flow by an active yaw system, and down consisting of a set of motors that rotate the nacelle and rotor around the vertical axis of the machine [2]. Power electronic converters are commonly used to control wind active and reactive power injected to grid (converters are usually located at ground level for maintainability). Local step-up transformer is usually installed next to each WTG for power transmission within the wind farm (cable reticulation of up to 10 km radial feeders) to MV collector substation.

Average wind farm installation cost is about ~2k US$/kW (2011) with foreseen reductions with R&D advances [2].

Four wind turbine generator technologies (listed hereunder) are commercially prevalent these days:

1- Fixed speed wind generators with squirrel cage induction generators.
2- Wind generators with wound rotor induction generators and limited speed variation through an external resistor.
3- Doubly Fed Induction Generators (DFIG) with variable speed.
4- Permanent Magnet Synchronous Machine or an Induction Machine (cage or wound rotor) with a full converter and variable speed range.

The most commonly used technology is the Doubly Fed Induction Generator (DFIG) [6]. This is due to the reduced converter capacity (~30% of machine rating) impacting positively the feasibility of high power installations.

Typical construction of DFIG is shown in Figure 2-2.

Power is injected to the grid by stator as well as the rotor through a double converter arrangement (Rotor Side Converter (RSC) & Line Side Converter (LSC)). DC chopper is used to control DC link voltages during operation as well as to limit power losses.

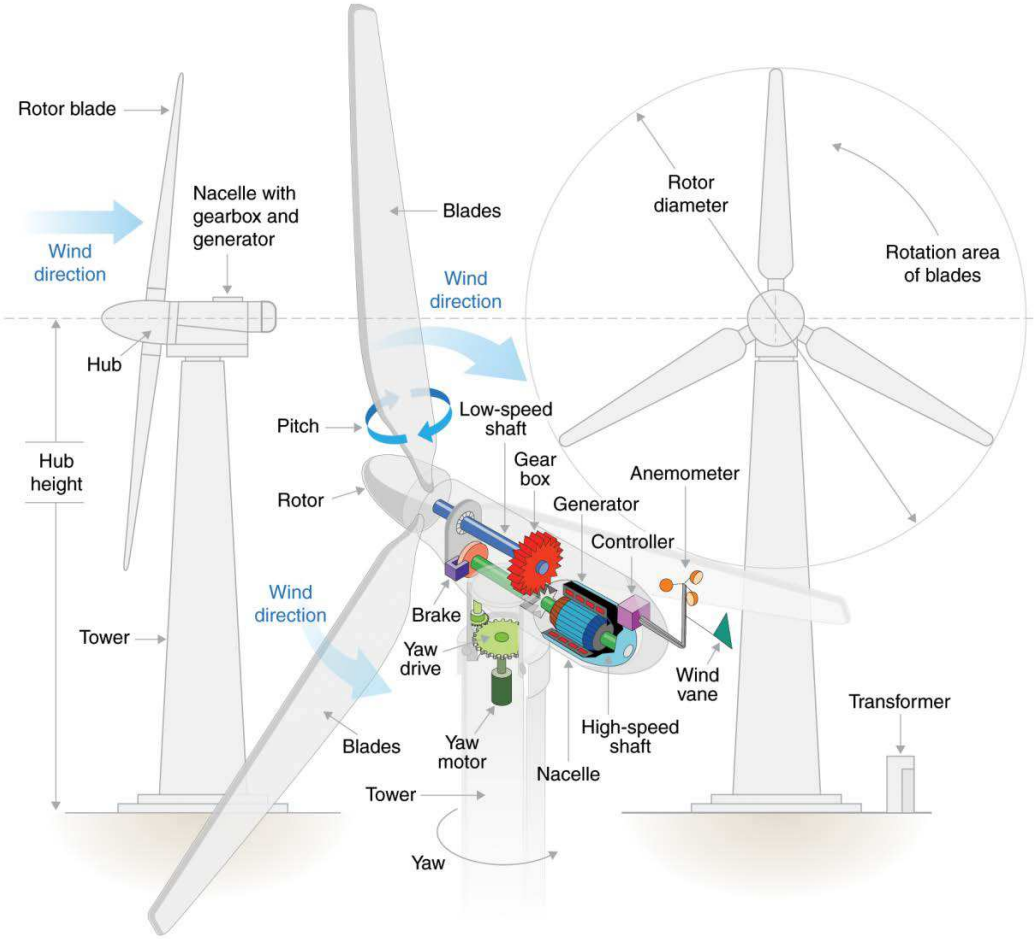


**Figure 2-1 : Typical modern horizontal axis wind turbine components [2].**

Due to the virtue of power electronic controllers, most DFIG designs have the capability to provide reactive power support to the grid. A vector control approach is utilized to split the rotor current into a *d*-axis (flux producing) component and *q*-axis (torque producing) component. Controlling the *d*-axis excitation on the rotor can achieve the reactive power support [6]. Switched electronic rotor crowbar is used to divert excessive currents.

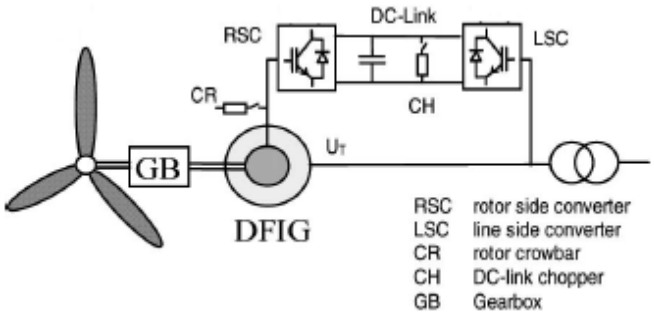


**Figure 2-2 : DFIG wind turbine schematic diagram [7].**

The reactive power support is very useful during voltage disturbances as it helps to retain system normal operating conditions quickly and improve system stability. Typical DFIG reactive power capability is show in Figure 2-3. (family of curves with different slip values "rotor speeds"). DFIG normally operates in the region bounded by red dash-dot lines. Green dots show the locus of unity power factor with no injection or consumption of reactive power.

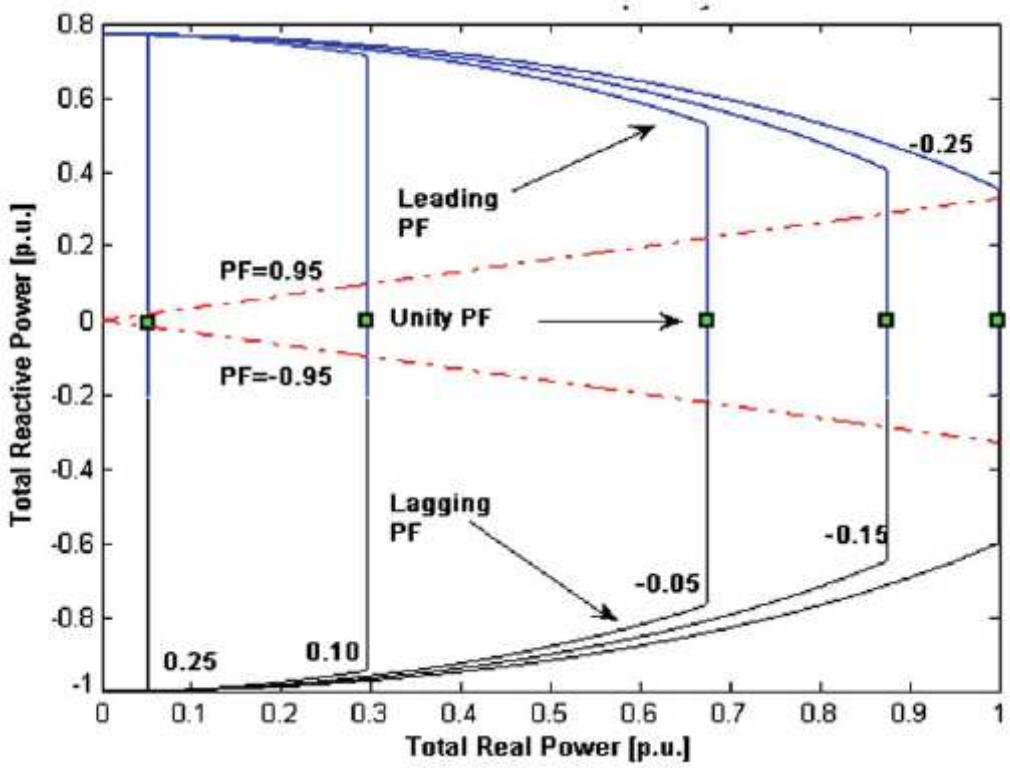


**Figure 2-3 : Reactive current capability at nominal voltage as a function of active current [6].**

### 2.2.1.1 Low Voltage Ride-Through (LVRT) Capability

Most of modern DFIG wind generators are provided with Low Voltage Ride-Through (LVRT) capability in order to utilize the DFIG reactive power support capability during voltage dips [8]. The reactive power support is important to avoid the risk of cascaded outages.

Typical LVRT capability requirements for various codes are shown in Figure 2-4. The reason behind local differences between codes is mainly to get use of the reactive power support capability of connected wind farms during system disturbances. The LVRT capability represents the capability of power converters to withstand transient heavy currents during voltage dips.

Grid requirement dictates the actual need for DFIGs LVRT capabilities during voltage variations. In this regard, induction generators are switched to the reactive power support mode if the PCC voltage drops beyond 10% of generator terminal voltage [9]. For example, German grid code (shown in red) asks for DFIGs to tolerate a zero voltage for about 150 ms and ramping up voltage to 90% at 1500 ms. The DFIG should be properly tuned and sufficiently capable of providing pre-selected "usually 2% of rated current for each percent of the voltage dip" reactive current during voltage recover not exceeding this pattern.

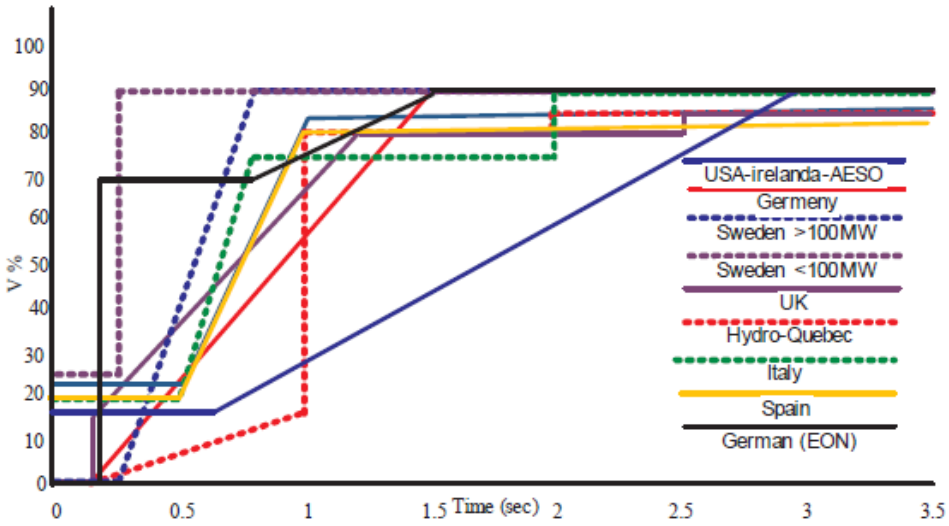


**Figure 2-4 : Wind farm fault ride-through requirement for various codes [9].**

### 2.2.1.2 High Voltage Ride-Through Capability (HVRT)

Similar to the LVRT operation, the wind farms have to provide reactive power support to the grid during High Voltage Ride-Through (HVRT) events. However, instead of delivering reactive power to the grid, reactive power should be absorbed during HVRT operation in order to mitigate the voltage rise/swell at PCC [10]. Figure 2-5 shows Germany (E.ON) and Spain HVRT requirements.

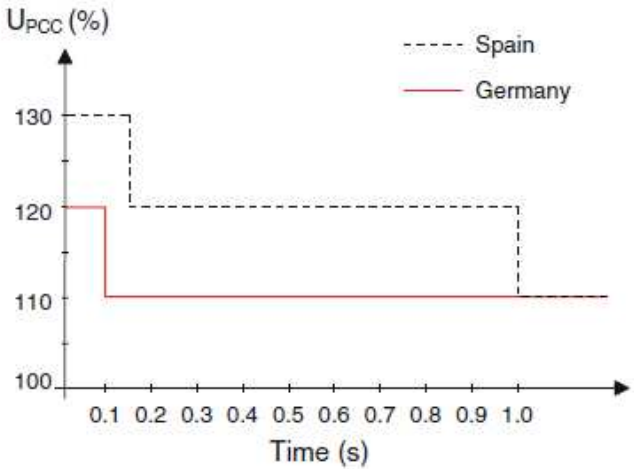


**Figure 2-5 : Wind farm HVRT requirement in Germany & Spain [10].**

### 2.2.2 Impact of Wind Generators on System Dynamic Performance

Wind generators impact on system dynamic performance has been an important subject of study as detailed in [9], [11], [12], [13] and [14]. The performance parameters under study are:

1- Frequency stability.
2- Rotor angle stability.
3- Voltage stability.

With a weak grid and isolated electrical systems, the integration of a large amount of wind generation may cause problems due to the limited capability of wind power generation systems to provide both the inertial rotating mass and the reactive current capacity to maintain stability after severe transient disturbances in the grid [13]. Basically, the high wind power gives rise to the fluctuations of the system frequency as the wind penetration increases. Fluctuations soar when exceeding beyond 10% of the total capacity [11]. With the virtue of modern power electronics, the injection of reactive power by WTGs (DFIGs) is possible. Reactive power support by DFIG improves the rotor angle response of grid synchronous generators during faults and system abnormalities [12].

### 2.2.3 Photovoltaic (PV) Systems

Photovoltaic technologies convert sunlight directly into DC electricity by enabling solar photons to “excite” electrons from their ground state, producing a freed (photo-excited) electron and a “hole” pair in semi conductive substrate (in most cases, silicone based). The electron and hole are then separated by an electric field that is formed by the design of the PV cell and pulled toward positive and negative electrodes, producing DC electricity. Figure 2-6 shows a typical PV construction [2].

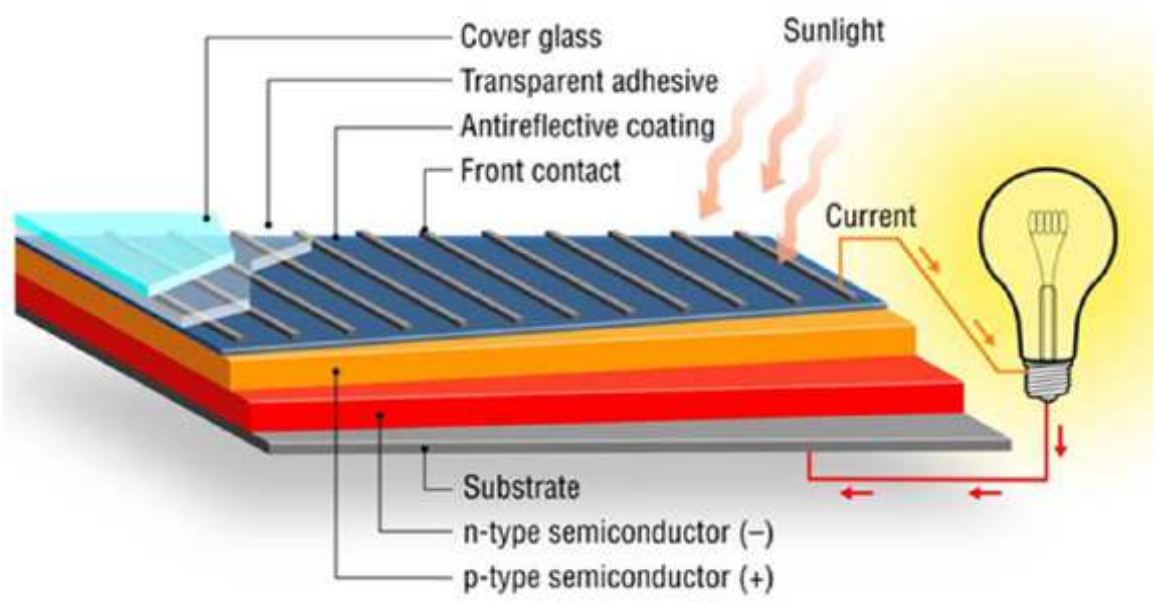


**Figure 2-6 : Typical PV cell construction**

PV generated DC power is controlled by a DC-DC converter usually supported by Maximum Power Point Tracking (MPPT) option to force the PV cell to operate at maximum power point. The DC-DC converter output is feeding a DC-link capacitor in turn feeds the DC/AC inverter. DC/AC inverter is used for AC power interface to distribution grid (Figure 2-7)

With the high cost impact of PV installations, economics plays major role in investment decision making. Recently, the PV installation costs are getting lower (around 2~3$/W) due to the advances in manufacturing and efficiency improvement [2].

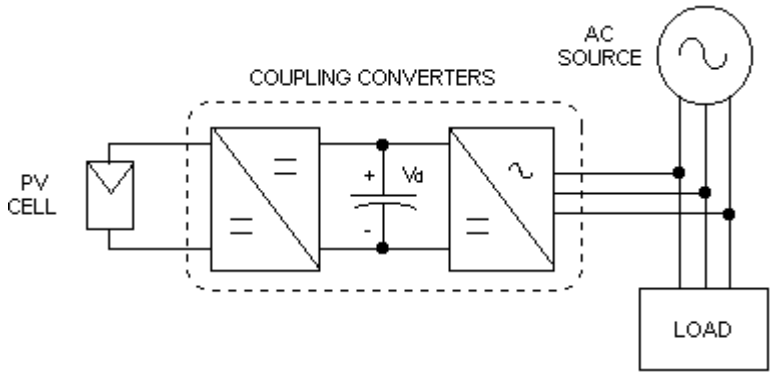


**Figure 2-7 : Grid-tied PV system [15].**

### 2.2.3.1 Low Voltage Ride-Through Capability (LVRT)

Due to the smaller share/penetration of photovoltaic (PV) systems in most of the operating power systems in the world, grid operators impose basic grid requirements. IEEE Std. 929-2000 recommends disconnection of PV systems during voltage disturbances exceeding certain limits (Figure 2-8) for safety reasons. Nevertheless, with the increased PV penetration, grid codes are expected to introduce LVRT requirement for MV and HV grid tied PV systems (Figure 2-9) [10].

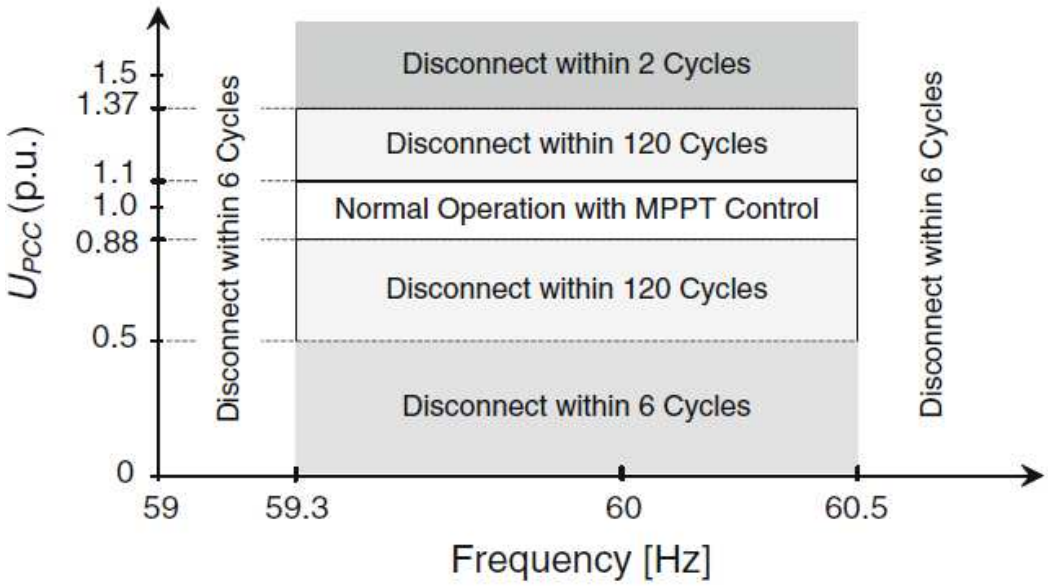


**Figure 2-8 : Voltage and frequency window for PV systems in IEEE Std 929–2000 [16].**

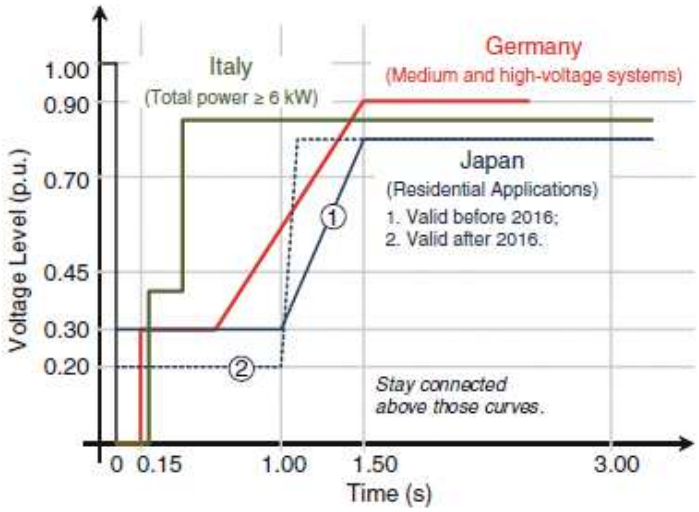


**Figure 2-9 : Example of the LVRT requirement in various countries [10].**

## 2.3 Voltage Disturbances

The study covers topics related with smart grid, renewable energy sources integrations, active and reactive power demand, system stability and operational abnormalities. References [9], [17], [18], [19] describe causes for voltage disturbances within grids to include:

- Faults (SLG is the most common).
- Motor starting.
- Load / generation rejection.
- Ferroresonance.
- Arcing ground faults.

Reference [17] gives a detailed description for various types of voltage disturbances and waveforms arising into modernized power systems due to the intensive presence of non-linear loads e.g. VFDs.

Consequences of supplying sensitive loads from networks borne to disturbances can result in outages, mal-operations and even damages. Examples of such cases are given in [3].

## 2.4 Active Voltage Quality Regulator (AVQR)

Active Voltage Quality Regulator (AVQR) is very similar in concept with AVC. Papers [20], [21] and [22] explain in detail the design and operational aspects of AVQR with different control techniques and topologies. No related papers can be located for researches carried out on grid impact of AVQR.

The AVQR topology/schematic as shown in Figure 2-10 resembles the ABB PCS100 AVC series outline topology. Injection transformer is used to impose corrective voltage component on supply voltages. Corrective voltage component is produced by controlled inverter connected to a rectifier driven DC link. The DC link voltage control technique causes a phase-shift between input and output voltages so that the resultant AVQR power is kept as minimum.

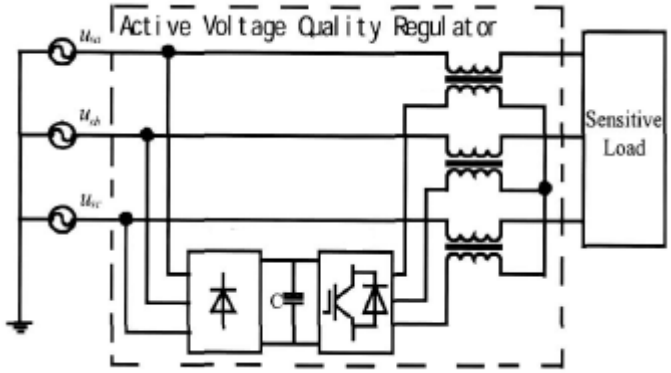


**Figure 2-10 : AVQR schematic as depicted in [22].**

## 2.5 Conclusion

Listed references of paper [22] don't deal with grid interface with AVQR. The AVC is a fairly new technology and no published titles can be located for research done on the impact of series active voltage conditioners on girds with high renewable energy penetration.

# 3 Active Voltage Conditioner (AVC)

## 3.1 Topology

The Active Voltage Conditioner (AVC) comprises of series boost transformer driven by precisely controlled rectifier/inverter set to compensate the grid voltage variations. Figure 3-1 shows the Single Line Diagram (SLD) of the PCS 100 AVC.

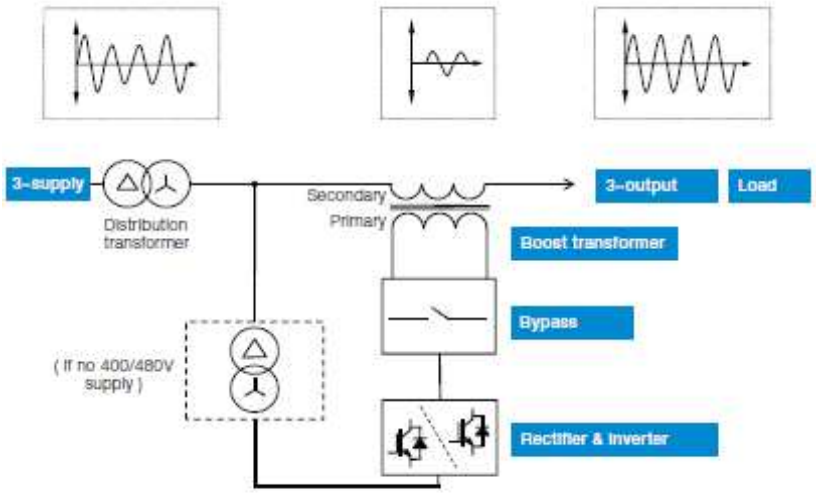


**Figure 3-1 : PCS100 AVC SLD & Waveforms [23].**

Injection/boost transformer (passive component of AVC) operates in its linear region by imposing additional or subtractive voltage wave on the grid waveform and accordingly keeping the output voltage stabilized. Figure 3-2 shows ABB installation in Germany for Medium Voltage PCS100 AVR. The unit is installed outdoor in a container enclosure with underground cable trenches. AVC enclosure size is proportional to its nominal power. The AVC power is limited to the product of voltage correction range (±10% typical) and nominal load current.

The AVC does not employ any energy storage devices e.g. battery, which enhances its minimal size and installation feasibility.

## 3.2 Operational Features

### 3.2.1 Concept

The PCS100 AVC has a nominal (guaranteed) correction range of ±10%. This is sufficient to compensate for voltage variation within most of grid operator codes worldwide.


**Figure 3-2 : PCS100 AVR (MV Level – Outdoor Installation)**

### 3.2.2 Efficiency

Being an active installation with only one passive power element (boost transformer), the AVC efficiency is very high (greater than 98%) [3]. Power loss is a function of loading and correction depth of the AVC. Figure 3-3 shows typical 400 kVA losses variation.

It is evident from Figure 3-3 that the losses increase with load current (resistive losses are proportional to the square of the current). Bypass losses is shown in green. AVC losses in connections and passive elements are shown in blue. The total losses including switching devices losses (active during correction) are shown in red.

### 3.2.3 Fast Operation

The AVC response time for voltage variations is typically as short as half a cycle [3]. This allows for the seamless operation to avoid disturbing sensitive process loads e.g. HVAC in chips manufacturing facilities. (Figure 3-4 shows the measured response of AVC to 30% and 50% voltage sags). Power quality improvement is achievable for wide range of sags and swells occurring for very short times to sustained overvoltage and undervoltages.

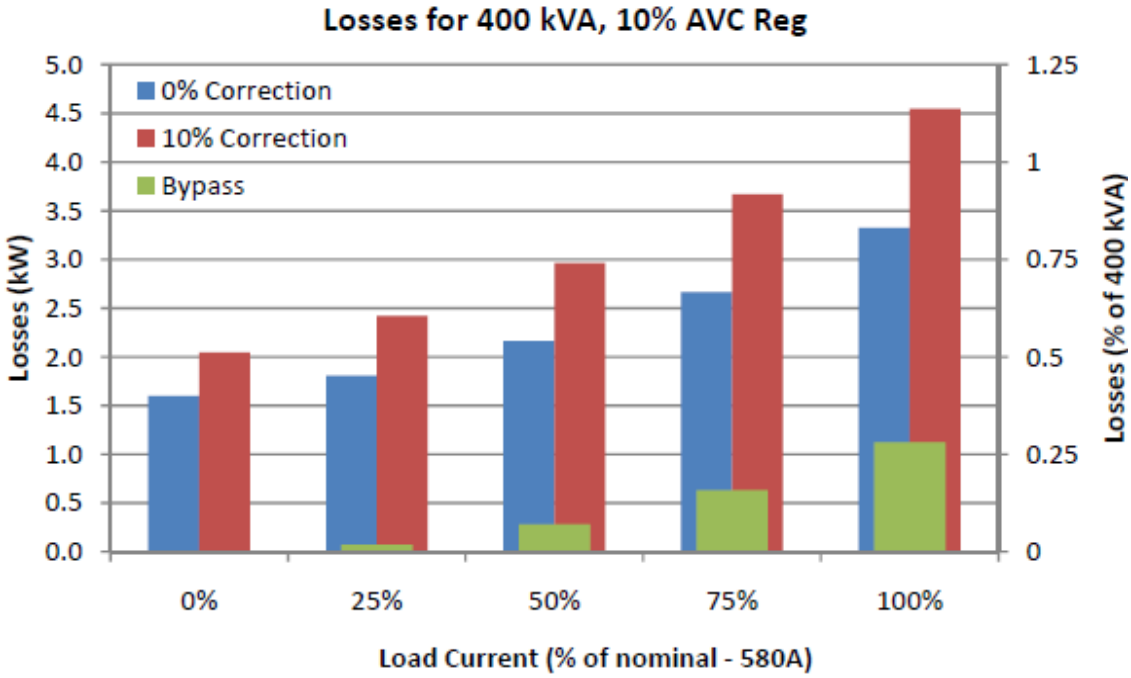


**Figure 3-3 : 400 kVA PCS100 AVC (LV) losses vs. loading**

The distribution transformers On-Load Tap Changers (OLTCs) are not fast enough to compensate for such short disturbances. This is due to slow Automatic Voltage Regulators (AVRs) response and mechanical moving parts inertia.

The fast response time allows modeling distributed AVCs connected to the same Point of Common Coupling (PCC) to respond collectively at the same time. Chapter 4 explains mathematical modeling of AVC grid interface.

The operation of AVC beyond ±10% is intermittent compared with a DVR (Dynamic Voltage Restorer) and supposed to last for few cycles as shown in (Figure 3-4) due to the lack of energy storage devices.

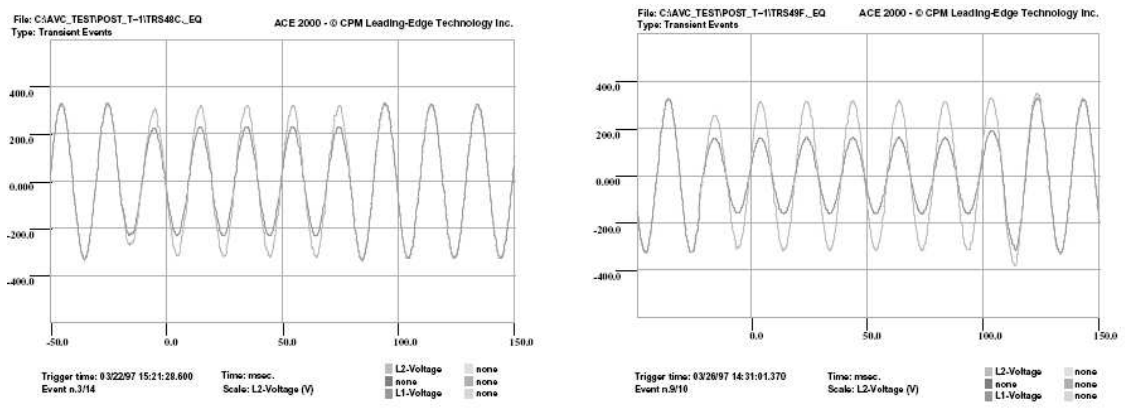


**Figure 3-4 : AVC response to 30% (left) & 50% (right) voltage sags – Volts. Vs. milliseconds [3]**

### 3.2.4 Waveform Conditioning

Waveform conditioning is also carried out by the AVC eliminating wave distortions and harmonics (other than zero sequence/triplen harmonics). This is usually limited to $11^{th}$ harmonic due to design constraints. Voltage Total Harmonic Distortion (THDv) input of up to 25% can be tolerated by PCS 100 AVR.

Sensitive power loads utilizing power electronics may well be subjected to mal-operation due to voltage waveform distortion due to zero crossing shift and EMI issues. AVC provides proper waveform/power quality for connected loads.

### 3.2.5 Through Fault Capability

PCS100 AVC introduces additional series impedance into network fault equivalent circuit. The downstream fault current is reduced by the boost transformer series impedance (ranging from 1 to 2%). There is no impact on zero-sequence impedance as the AVC is a three-wire system and the injection transform is connected in series with the current loop.

Due to design economics, the AVC does not have deliberate means for reducing through-fault currents. The inverter is usually bypassed during heavy fault currents. A fast acting silicone controlled rectifier bypass on the inverter side is enabled by AVC overcurrent protection when the current exceeds 2 p.u., this in turn is bypassed by mechanical contacts.

The same technique is used in case of AVC internal fault.

### 3.2.6 Unsymmetrical Voltage Conditioning

Single phase faults cause voltage dips on faulty phases and voltage swells on healthy phases depending on system neutral point grounding connection. Most of MV networks have their star points grounded through Neutral Grounding Resistors (NGR) to limit the system single phase-to-ground fault current, while LV networks usually have solidly grounded configuration to allow for single phase loads.

The phase-to-ground faults are very common on industrial and commercial networks (about 98% of industrial system faults are single phase-to-ground) causing zero sequence current and voltage components to exist within the system (if a neutral current path exists). Nevertheless, the PCS100 AVC doesn’t compensate for zero sequence voltages.

In the case of faults on an 11 kV network (usually an NGR is provided), voltages (to ground) on healthy two phases will jump to line-to-line values causing additional stresses on system insulation and cabling (Figure 3-5).

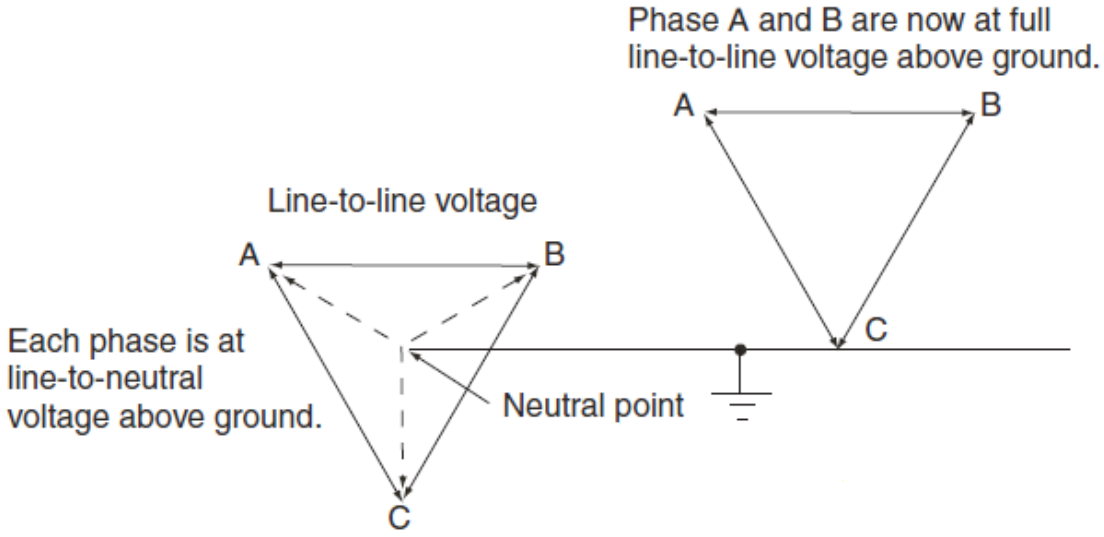


**Figure 3-5 : Phase relationships during normal and faulty conditions (Neutral Grounded through Impedance)**

The AVC will not compensate for the phase voltages. AVC line-to-line output voltages will be compensated properly (resultant zero sequence voltages diminish for line-to-line voltages). Eqs.(3-1) demonstrate the diminishing of zero sequence components in line-to-line voltages.

$$\begin{bmatrix} V_a \\ V_b \\ V_c \end{bmatrix} = \begin{bmatrix} 1 & 1 & 1 \\ a^2 & a & 1 \\ a & a^2 & 1 \end{bmatrix} \cdot \begin{bmatrix} V_1 \\ V_2 \\ V_0 \end{bmatrix}$$

$$\Rightarrow V_{ab} = V_b - V_a = V_1\left(1-a^2\right) + V_2(1-a)$$

$$V_{bc} = V_c - V_b = V_1\left(a-a^2\right) + V_2(a^2-a)$$

$$V_{ca} = V_a - V_c = V_1(1-a) + V_2(1-a^2) \qquad (3\text{-}1)$$

$$\Rightarrow \begin{bmatrix} V_{ab} \\ V_{bc} \\ V_{ca} \end{bmatrix} = \begin{bmatrix} V_b - V_a \\ V_c - V_b \\ V_a - V_c \end{bmatrix} = \begin{bmatrix} \left(1-a^2\right) & (1-a) & 0 \\ \left(a-a^2\right) & (a^2-a) & 0 \\ (1-a) & (1-a^2) & 0 \end{bmatrix} \cdot \begin{bmatrix} V_1 \\ V_2 \\ V_0 \end{bmatrix}$$

$$a = 1\angle 120°$$

where $V_a$, $V_b$, $V_c$ are phase-to-neutral voltages, $V_{ab}$, $V_{bc}$, $V_{ca}$ are line-to-line voltages.

The operation of AVC on resistor grounded network will achieve the line-to-line compensation (no zero sequence involved) while phase-to-ground voltages will not be compensated due to the presence of zero sequence current and voltage components

during system unbalances and faults. Delta-star transformer can be used past the AVC to achieve conditioned phase-to-ground voltages. Review of network fault current setting may be needed to accommodate additional system impedance (boost transformer).

## 3.3 PLECS/Simulink Simulation

### 3.3.1 Model

ABB NZ have provided simplified PLECS/Simulink model for AVC. PLECS® is a tool for high-speed simulations of power electronic systems [24]. Figure 3-6 shows rectifier-inverter link injects compensating voltages into the source voltage through boost/injection transformer (represented as a linear inductance). Control signals are derived mathematically using Park and Clarke reference frame transformations with a reference signal (pure sinusoidal positive sequence at power frequency) and power limit. Phase Locked Loop (PLL) is employed to synchronize injection inverter to the grid.

The model uses normalized per unit values for ease of application. Further technical details of the model may be requested on ABB NZ discretion.

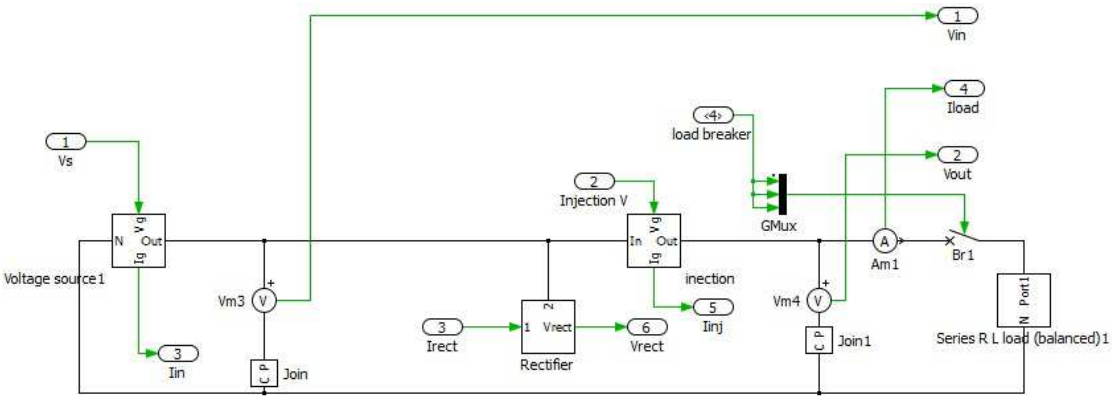


**Figure 3-6 : PLECS model for ABB AVC**

### 3.3.2 AVC Response to Undervoltages

A 10% undervoltage ($V_{PCC}$) is simulated using PLECS/Simulink model. Voltage sag is compensated in about half a cycle keeping the load voltage quickly at nominal value. Load current is also kept at nominal value; nevertheless, the source current sees an increase to keep the load power constant because the instantaneous power is the

product of voltage and current. It is noted that the supply power factor is almost equal to load power factor (initial ramp in Figure 3-7 is due to PLECS numericals).
Figure 3-7 shows AVC PLECS model waveforms for 10% undervolage.

### 3.3.3 AVC Response to Overvoltages

Similarly, a 10% overvoltage ($V_{PCC}$) is simulated using PLECS/Simulink model. Since the load power is proportional to the load voltage (constant, when conditioned), the load power is constant, while source voltage swells, the source current decreases to keep the constant load power demand. It is noted that the supply power factor is almost equal to load power factor (initial ramp in Figure 3-8 is due to PLECS numericals).
Figure 3-8 shows AVC PLECS model waveforms for 10% overvoltage.

For discussion of simulation results and mathematical details related to this section, please refer to Chapter 4.

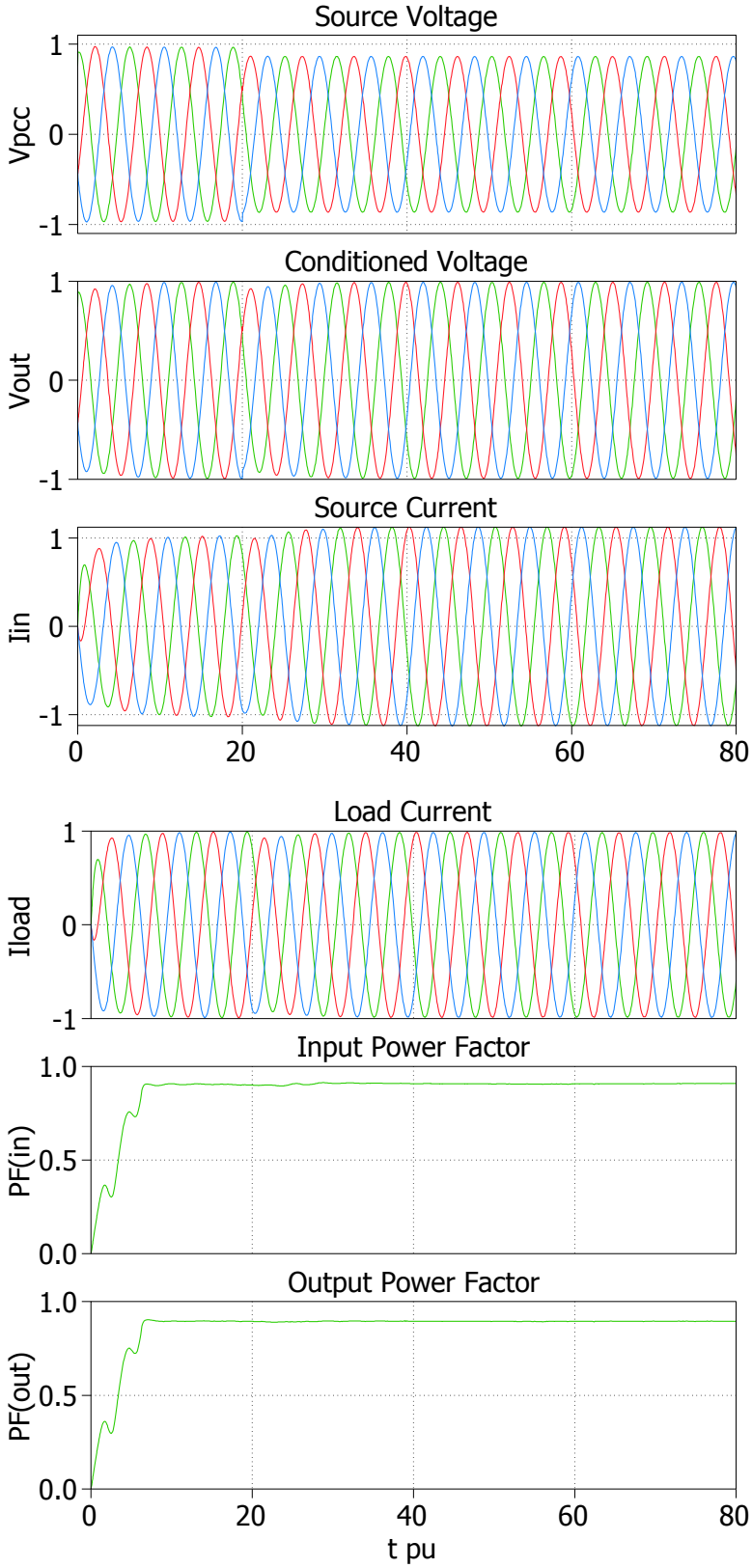


**Figure 3-7 : AVC response with 10% voltage sag (PF =90%).**

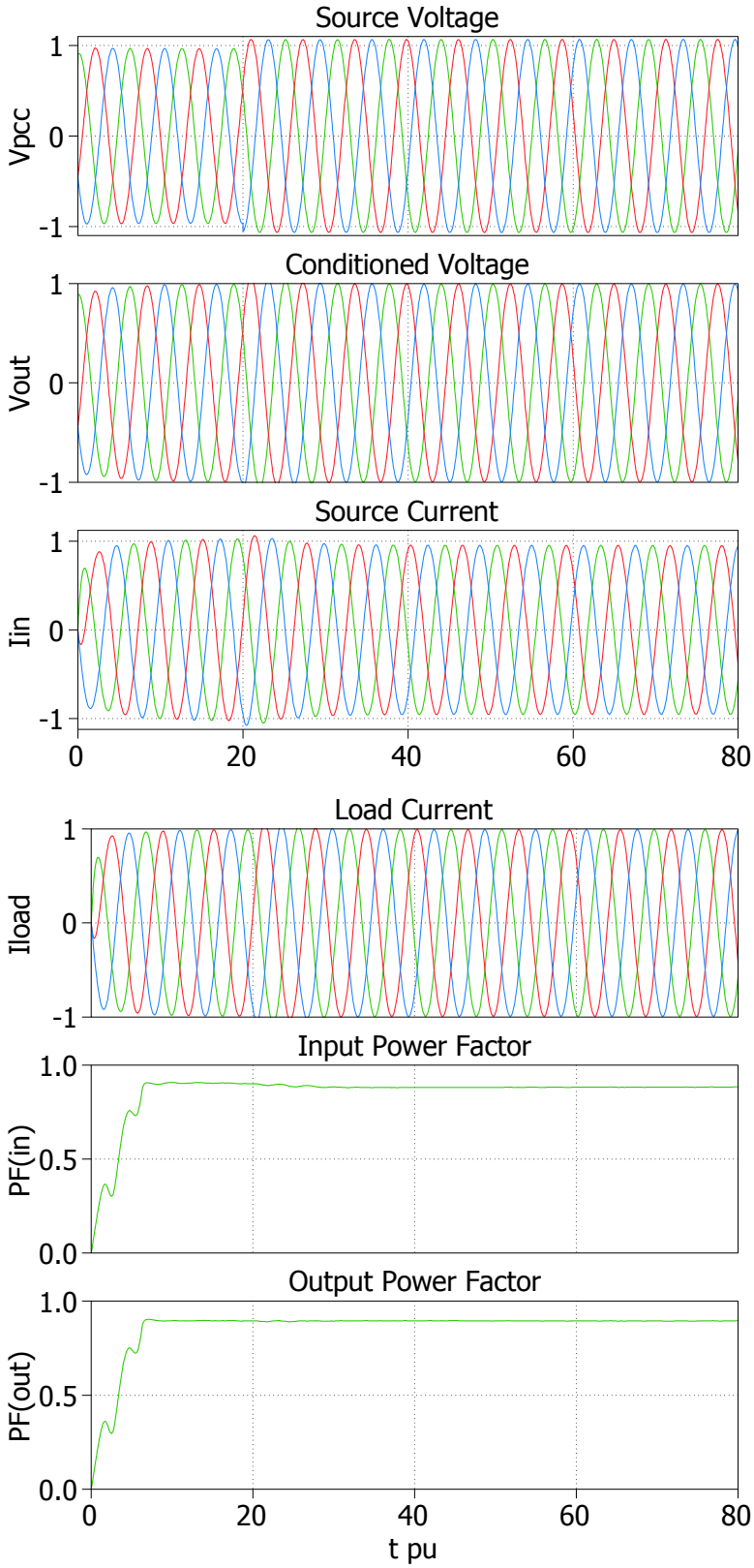


**Figure 3-8 : AVC response with 10% voltage swell (PF =90%).**

# 4 AVC-Grid Interaction

## 4.1 Simulations Analysis

PLECS® simulations confirm the power/energy conservation concept. Undervoltages cause increase in grid current (demand) while overvoltages cause line currents to decrease. This concept is the basis for the AVC impact mathematical modeling in this chapter.

The derived equations are based on 3-phases system notations. Most of the involved parameters are vector quantities. Given that the operation of AVC doesn't change the load/supply power factor as shown in Figure 3-7 and Figure 3-8, linear algebraic addition is used.

## 4.2 Operation of AVC during Voltage Disturbances

The Active Voltage Conditioner (AVC) compensates the voltage variations as seen on PCC keeping the load power constant over the correction range (±10%).

As shown in Figure 3-7 and Figure 3-8, the AVC input power factor is almost equal to its output (load) power factor; this allows the linear algebraic equations for analyzing the additional currents associated with AVC operation.

During an undervoltage event due to any operational disturbance like system undervoltage, heavy motor starting, generation rejection/fluctuation, remote fault,…etc, the AVC keeps the load voltage constant (@ $V_n$ p.u.) and accordingly, the demand power (@$S_n$ p.u.). Given that the AVC does not have any energy storage capability and has very high efficiency; the grid "sees" a constant load power demand during the event.

Since the AVC has a very short response time to input voltage disturbances, it can be presumed that all connected AVCs on the same PCC responds at the same time. (Figure 4-1).

### 4.2.1 PCC with 100% Conditioned Loads

Let the aggregate AVC conditioned loads to be represented as a linear load with constant impedance $Z_c$, and nominal system line-to-line voltage $V_n$, the demand power can be represented by Eq.(4-1).

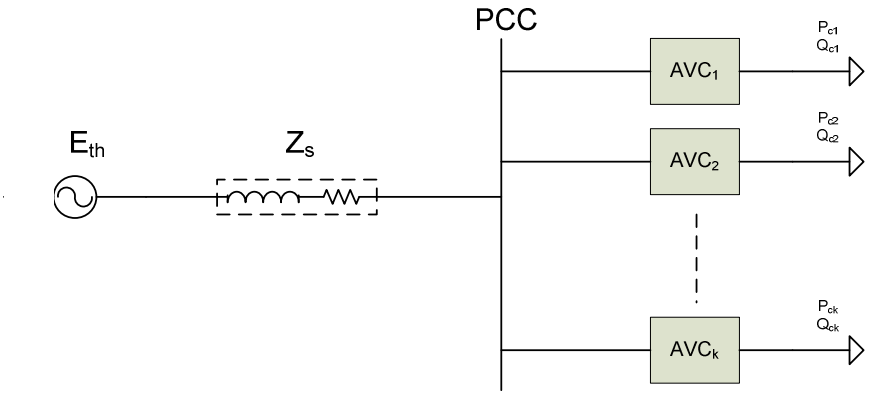


**Figure 4-1 : Typical distribution bus with *k* connected AVCs.**

$$\left\{\begin{array}{l} S_{AVC} = \dfrac{V_n^2}{Z_c} \\ P_{AVC} = \sqrt{3} V_n I_n \cos\phi \\ Q_{AVC} = \sqrt{3} V_n I_n \sin\phi \end{array}\right\} \qquad (4\text{-}1)$$

Where,

$$\frac{1}{Z_c} = \frac{1}{Z_{c1}} + \frac{1}{Z_{c2}} + \frac{1}{Z_{c3}} + ..... + \frac{1}{Z_{ck}} = \sum_{i=1}^{k} \frac{1}{Z_{ci}}$$

This demand is constant over voltage variation range of $0.9V_n$ to $1.1V_n$.
Voltage deviations from nominal voltage $V_n$ is represented by differential voltage $\Delta V$ as per Eq.(4-2).

$$V_{PCC} = V_n - \Delta V \qquad (4\text{-}2)$$

In case of no AVC installed, the demand power varies proportionally with the square of the system voltage and inversely with the load impedance:

$$S_g = \frac{V_{PCC}^2}{Z_c} = \sqrt{3} V_{PCC} I_g \qquad (4\text{-}3)$$

And the grid current will be:

$$I_g = \frac{V_{PCC}^2}{\sqrt{3}Z_c} \qquad (4\text{-}4)$$

From Eq. (4-4), during a voltage disturbance, the demand power and grid current follow the system voltage in case of no AVC installed, Nevertheless; with AVC in action, the demand power remains constant (equal to $S_{AVC}$) forcing the grid supply current to deviate from its value in case of no AVC.

Rewriting Eq. (4-4) :

$$I_g = \begin{cases} \dfrac{S_n}{\sqrt{3}V_g} = I_{g-AVC} \ldots 0.9V_n \le V_g \le 1.1V_n \\ \dfrac{V_{PCC}}{\sqrt{3}Z_c} \ldots\ldots\ldots\ldots\ldots\ldots Elsewhere \end{cases} \qquad (4\text{-}5)$$

Plots hereunder in (Figure 4-2) depict the AVC impact on load linearity versus PCC voltage. Most of loads are considered as constant impedance load (linear), where the V-I characteristics are linear with slope representing the reciprocal of load impedance. AVC transforms the loads into a constant power/demand load around the conditioning voltage range (±10%) as shown in Figure 4-2.

A spike in grid current is observed at -10% voltage (dip) in order to keep the load power constant.

The inverse gradient passes the nominal voltage (100%) point at nominal current i.e. 0% AVC conditioning. A shallow current demand appears at +10% voltage (swell) to intersect with the linear load characteristics again. AVC piece-wise V-I characteristics may be extended beyond ±10% of nominal voltage for very short time.

The equations and graphs are valid for the 100% PCC conditioned loads case.

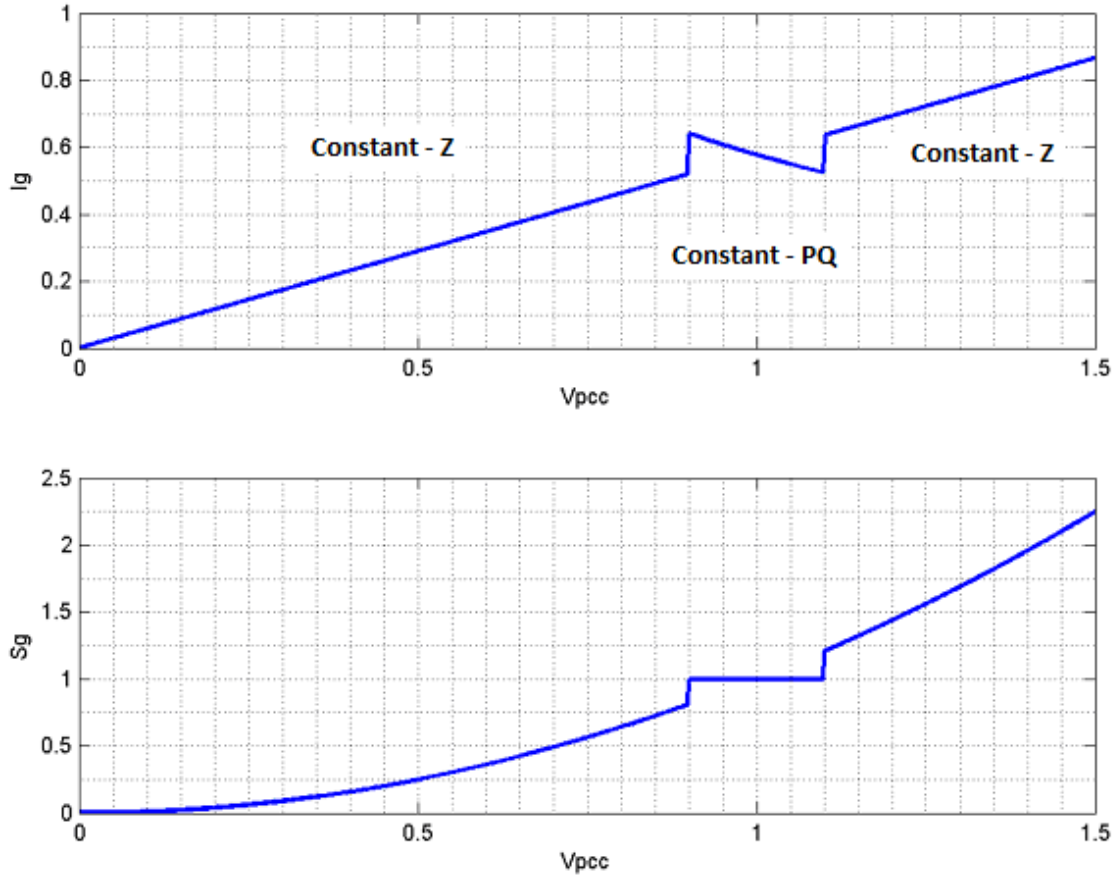


**Figure 4-2 : AVC V-I characteristics and complex power variation with applied voltage.**

## 4.2.2 PCC with Mixed Loads

Realistically, some users may still tie their loads to the grid with no AVC and their demand follows Eq. (4-3). Equivalent network is shown in Figure 4-3.

With mixed loads, $S_c$ is the conditioned load demand and $S_{uc}$ is unconditioned load demand, the *conditioning ratio x* can be defined as the ratio between conditioned load demand $S_c$ and the total connected load $S_t$ at PCC.

$$x = \frac{S_c'}{S_{uc} + S_c} \tag{4-6}$$

$$S_t = S_c' + S_{uc} \tag{4-7}$$

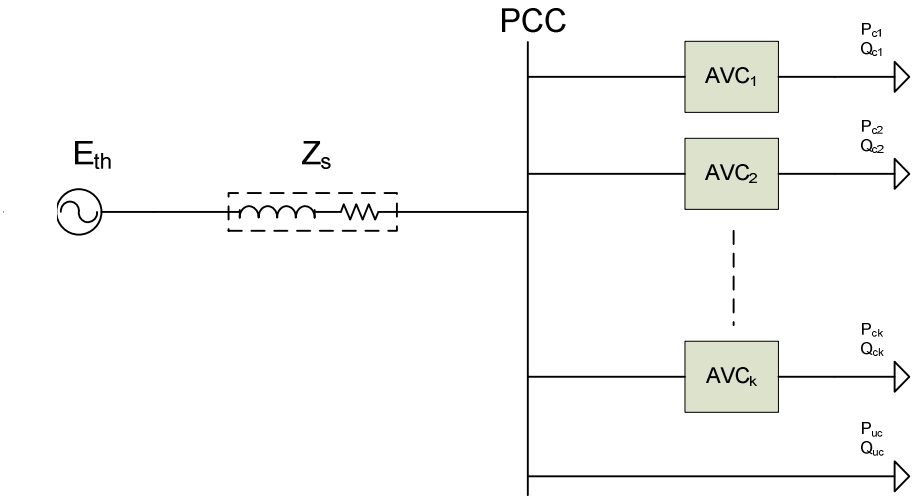


**Figure 4-3 : Typical distribution bus with k connected AVCs and unconditioned loads.**

Additional grid supply current due to AVC $\Delta I_g$ can be represented as:

$$\Delta I_g = \frac{xS_t}{\sqrt{3}}\left[\frac{1}{(V_n - \Delta V)} - \frac{(V_n - \Delta V)}{V_n^2}\right] \qquad (4\text{-}8)$$

With values above in per unit, assuming $V_n$=1 p.u., Eq. (4-8) becomes:

$$\Delta I_g = \frac{xS_t}{\sqrt{3}}\left[\frac{\Delta V(2 - \Delta V)}{1 - \Delta V}\right] \qquad (4\text{-}9)$$

Figure 4-4 plots the dependency of additional grid current on conditioning ratio *x* and voltage variation ΔV. Positive ΔV refers to PCC undervoltage. (Refer to Eq. (4-2)). Values greater than 0.1 p.u. voltage variations are true (theoretically) for short intermittent AVC operations.

It is clear that the greater the conditioning ratio, the higher the additional grid current demand. The above equations neglect the additional voltage drop caused by grid impedance and additional grid supply current $\Delta I_g$.

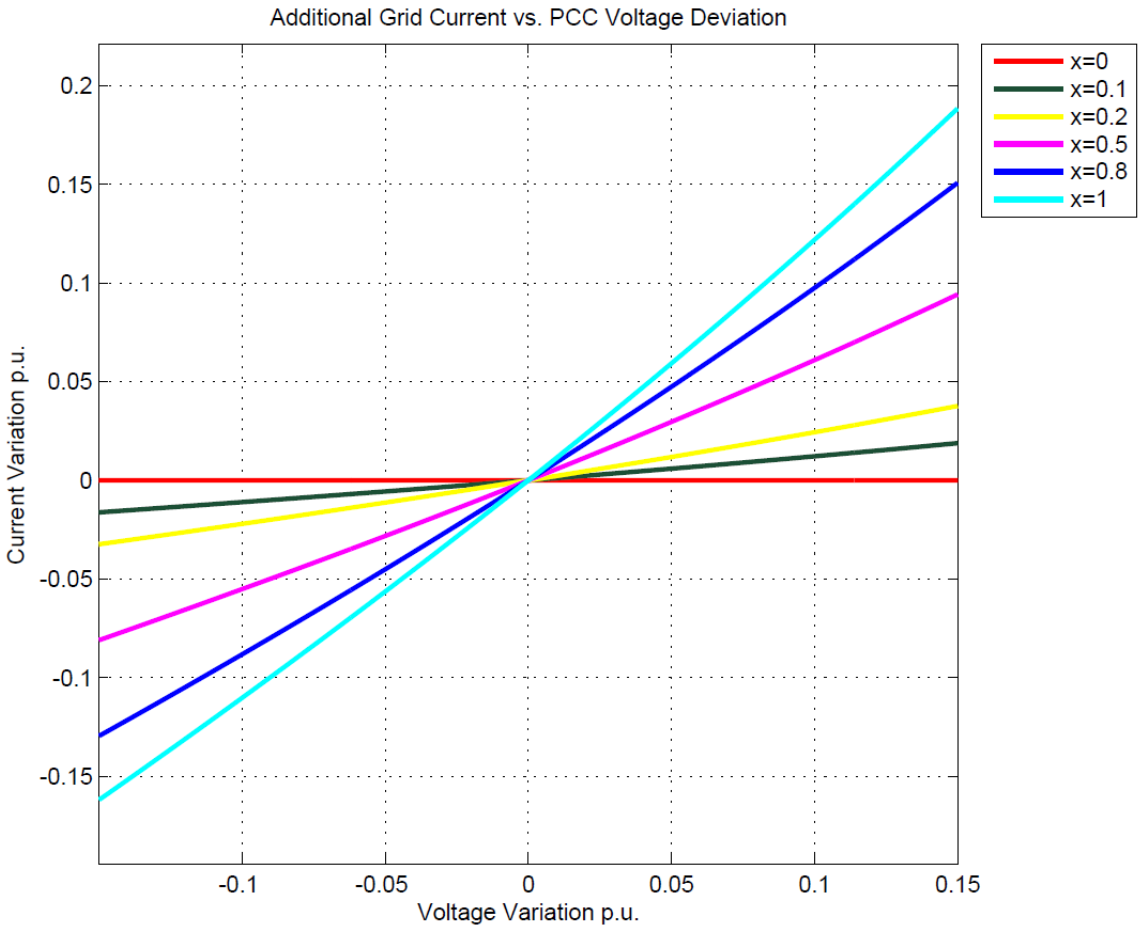


**Figure 4-4 : Additional grid current ($\Delta I_g$) due to AVC operation vs. voltage variation ($\Delta V$) "*x*=0 : no AVC".**

### 4.2.3 Impact of Weak Grid Stiffness

Most of remote radial load centers/consumers are subjected to low grid short circuit currents. Additional voltage drop due to additional current causes further shift of the operating PCC voltage. The grid equivalent stiffness described by $Z_s$ can hint about the available PCC short circuit current and associated amount of additional voltage increase/decrease due to AVC operation.

#### 4.2.3.1 Analytical Solution

Due to the linear nature of supply grid reactance and resistance, superposition can be used to estimate the additional voltage drop $\Delta V_a$ can be based on Eq.(4-9) while Eq. (4-2) will be:

$$V_{PCC} = V_n - (\Delta V + \Delta V_a) \qquad (4\text{-}10)$$

Thus,

$$\Delta V_a = \sqrt{3}\Delta I_g Z_s = Z_s x S_t \left[\frac{1-(1-\Delta V-\Delta V_a)^2}{1-\Delta V-\Delta V_a}\right] = x\frac{S_t}{S_{sc}}\left[\frac{1-(1-\Delta V-\Delta V_a)^2}{1-\Delta V-\Delta V_a}\right] \quad (4\text{-}11)$$

where $S_{sc}$ is the system short circuit VA (p.u.) @ PCC.

$\Delta V_a$ can be determined iteratively. For power quality reasons associated with intermittent power fluctuations, some countries have defined for wind farms a short circuit level at the connection point between 20 and 25 times the wind farm capacity. Lower short circuit levels have been already in operation within some networks [25]. Considering a value of 20 as the SCR for the equivalent grid stiffness and substituting in Eq.(4-11) for $\Delta V_a$ yields:

$$\Delta V_a = 0.05x\left[\frac{1-(1-\Delta V-\Delta V_a)^2}{1-\Delta V-\Delta V_a}\right] \quad (4\text{-}12)$$

As shown in Table 4-1, Table 4-2 and Table 4-3, additional voltage depends on the initial voltage variation $\Delta V$ and conditioning ratio *x*. It is clear that the greater the conditioning ratio, the higher the additional grid voltage variation. The AVC does not operate beyond ±10% and thus, voltage at PCC cannot exceed the correction limits (±10%), cells with PCC voltages exceeding +10% or -10% value (theoretically) are coloured in red and blue, respectively.

Due to the inverse gradient curve representing the constant power load, $V_{PCC}$ response to undervoltages appears to be greater than that during overvoltages. This is clear when comparing the absolute value/magnitude of additional voltage with initial voltage variation of 8% (Undervoltage) and 8% (Overvoltage) in Table 4-1 (highlighted in yellow). The difference becomes less noticeable with lower initial variations and conditioning ratios. Figure 4-5 shows the difference between response magnitude percentage due to overvoltages (O/V) and undervoltages (U/V). The impact of equivalent grid stiffness on additional voltage can be obtained by plotting

$\Delta V_a$ from Eq.(4-11) against equivalent grid Short Circuit Ratio (SCR) as shown in Figure 4-5.

Note that these curves in Figure 4-5 are clipped at a total PCC voltage variation of 10% (magnitude) since the AVC acts at that limit. With initial voltage variation of 5%, absolute values of $\Delta V_a$ greater than 5% to be clipped and at 7.5% initial variation, absolute values of $\Delta V_a$ greater than 2.5% to be clipped

Accordingly, additional reactive power demand as seen by the upstream supply is given by Eq.(4-13):

$$\begin{aligned}\Delta Q_g &= Q_{AVC} - Q_{No\ AVC} = \left[\frac{V_n^2}{Z_c} + \frac{\left(V_n - \Delta V - \Delta V_a\right)^2}{Z_{uc}}\right].\sin\phi - \frac{\left(V_n - \Delta V\right)^2}{Z_t}.\sin\phi \\ &\approx S_t\left(2x\Delta V - x\Delta V^2 + 2(x-1)\Delta V_a\right).\sin\phi\end{aligned} \tag{4-13}$$

### 4.2.3.2 Graphical Solution

#### 4.2.3.2.1 100% Conditioning

AVC Operational voltage can be determined by means of graphically solving both source and load V-I characteristics. Kirchhoff's Voltage Law (KVL) applied to Thévinin equivalent circuit in Figure 4-1 for supply gird results in Eq.(4-14).

$$E_{th} - \sqrt{3} I_g Z_s = V_{PCC} \tag{4-14}$$

Eq.(4-14) may be represented as a load line intersecting with AVC V-I characteristics in Figure 4-2.

In Figure 4-1, Thévinin equivalent EMF ($E_{th}$) depends on the system topology; Convenient representation of $Z_s$ in network planning usually uses bus/PCC short circuit capacity (~MVA) or available short circuit current (~kA).

Rewriting Eq.(4-14) :

$$I_g = \frac{\sqrt{3} Z_s I_f - V_{PCC}}{\sqrt{3} Z_s} \tag{4-15}$$

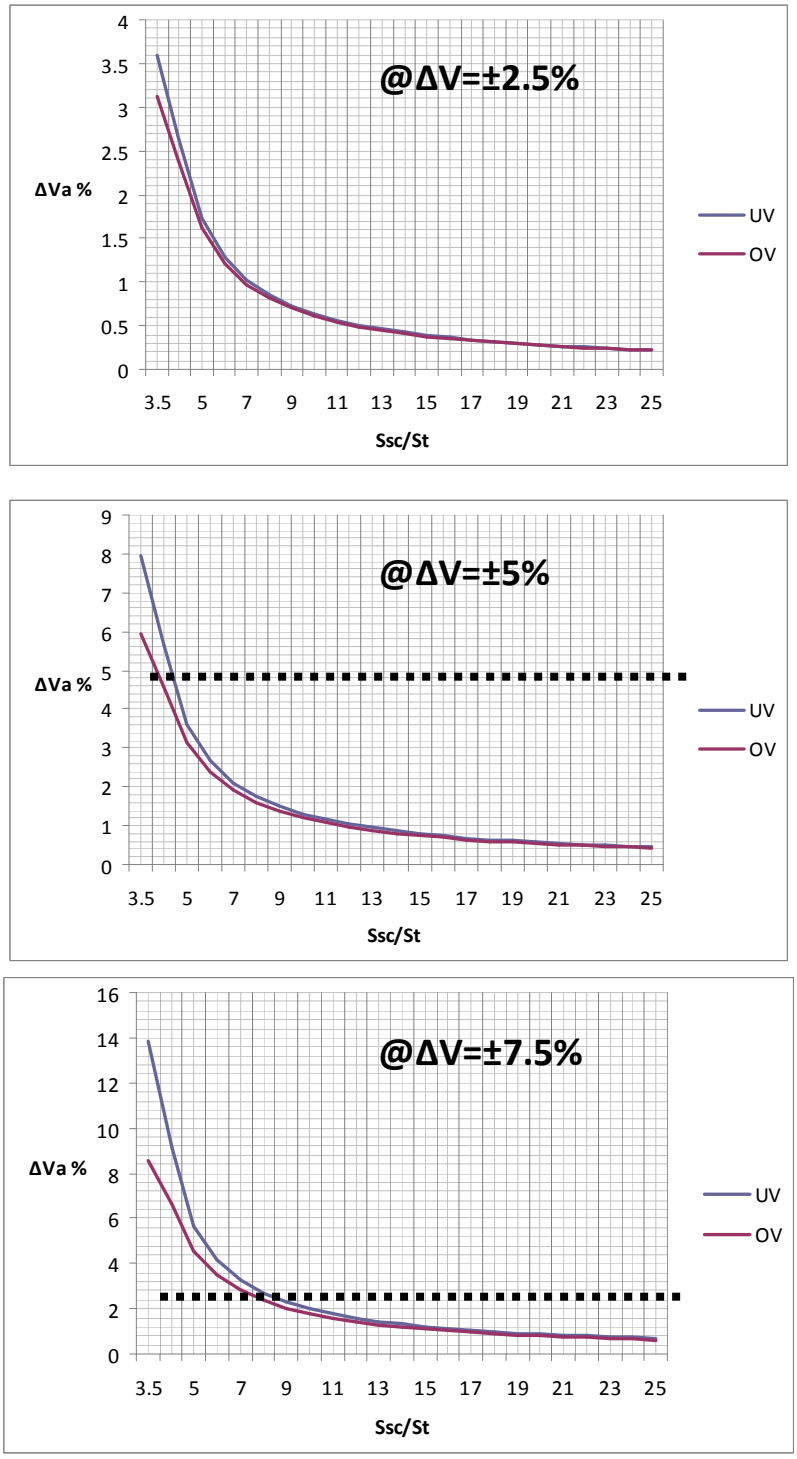


**Figure 4-5 : Additional voltage vs. equivalent grid SCR.**

Plotting both equations (4-5) and (4-15) in Figure 4-6 for a 380 V PCC with AVC conditioning a load of 50 kVA. During normal operation, the load lines representing two grid stiffness (5 kA & 15 kA) passes through the same operating point of $V_n$ & $I_n$.

Undervoltage of 7% (without AVC) causes a shift in PCC voltage value of about 2.28 V(0.6%) with 2 kA available short circuit current and about 0.86 V (0.225%) with 5 kA grids. Overvoltages also cause further shift (due to reduced current demand). 7% overvoltage (without AVC) causes a shift in PCC voltage value of about 2.1 V (0.55%) with 2 kA available short circuit current and about 0.8 V (0.21%) with 5 kA grids. These values conform to analytical results as detailed in 4.1.

#### 4.2.3.2.2 Mixed Loads

Similar to 100% conditioning, the AVC V-I characteristics are modified to incorporate portion of the PCC load following the system voltage without conditioning. The lower the conditioning ratio, the lower the additional voltage. (Figure 4-7).

## *4.3 AVC Impact on connected sources*

### 4.3.1 Impact Mechanism

As demonstrated in 4.2 , the AVC interaction during voltage variations on PCC causes:

a- Constant demand

b- Additional/subtractive current (and voltage)

The impact of AVC operation on grids with high renewable energy sources can be predicted based on the response of individual renewable source to bus voltage disturbances and demand variations. Nevertheless, and due to the stochastic nature of renewable energy, it is difficult to estimate the impact on overall wide spread smart grid with high penetration of renewable energy sources.

Impact of additional PCC voltage variation can be investigated on wind farms and PV plants separately. With steeply increasing installation rate of wind turbine generators (WTGs), the Doubly Fed Induction Generators (DFIGs) are the most common type used for this application. Versatile control methods of DFIG enable controlling reactive power injected into the grid and encourage keeping the wind farms connected to the grid during voltage variations in order to provide voltage support. Additional voltage variations directly affect the ride-through requirements for WTGs as explained in 2.2.1.1 and 2.2.1.2.

Comparatively, a similar impact can be predicted on the Photovoltaic installations as explained in 2.2.3.1.

### 4.3.2 Additional Voltage Variation due to AVC Operation

As highlighted above, additional voltage variation takes place due to the operation of AVC. This can be the major impact at PCC voltage directly related to the AVCs.

When a generator injects power into the network, the voltage tends to rise. In HV networks, this phenomenon occurs mainly when reactive power is injected because the line resistance is negligible compared with the line inductive reactance [5]. Instead, in MV & LV distributed networks, the line resistance is not negligible, thus an active power injection increases the voltage. Accordingly, the so-called "decoupling", which is typical of HV networks, cannot be applied in MV & LV networks. The variations are "coupled" with the voltage variations [5]. For the model under study, the simplified equivalent circuit in Figure 4-1 and Figure 4-3 is used.

### 4.3.3 Wind Farms Performance during Voltage Disturbances

As detailed under 2.2.1.1 and 2.2.1.2, the LVRT and HVRT requirements represent the required reactive power support required on Point of Common Coupling (PCC) of wind farms.

### 4.3.3.1AVC Contribution

As detailed in 4.2, the AVC causes additional voltage variation making the voltage dip/undervoltage to go deeper and the overvoltage to go higher due to the stabilized load demand. The impact is not symmetrical around system nominal voltage but with undervoltages causing greater additional voltage when compared with overvoltages with equal magnitudes.

An additional voltage of up to 1% may be present during voltage recovery. Notwithstanding that, the AVC contribution does *not* cause operational voltage variations to exceed ±10% regardless of equivalent grid stiffness; this can be verified as detailed under clause 4.1, Figure 4-6 and Figure 4-7.

When the PCC voltage reaches ±10%, the load line intersects with the V-I characteristics at ±10% without any additional variations compared with other values over the range of $0.9V_n$ to $1.1V_n$. Most grid codes have no requirement for both

LVRT and HVRT capability into the ±10% region as shown in Figure 2-4 and Figure 2-5, respectively.

It can be concluded that the AVC has *no direct effect* on the LVRT or HVRT requirements for coupled WTGs. Shifting the operational Point of Common Coupling (PCC) voltage impacts the power flow capability of connected WTGs. Most of modern DFIGs are normally operating within ±10% range and no major impact due to AVC operation can be envisaged.

Initial variation

| | $\Delta V$ (pu) % | $S_t=S_n$ (pu) | $S_c$ (pu) | $S_{uc}$ (pu) | $S_{sc}$ (pu) | x | $\Delta I_g$ (pu) | $\Delta V_a$ (pu) | $V_{pcc}$(final-Calculated) | $V_{pcc}$(final-Actual) | $\Delta V_a$ (updated) |
|---|---|---|---|---|---|---|---|---|---|---|---|
| Undervoltage | 10 | 1 | 1 | 0 | 20 | 1 | 0.122 | 0.012 | 0.888 | 0.900 | 0.000 |
| | 9 | 1 | 1 | 0 | 20 | 1 | 0.109 | 0.011 | 0.899 | 0.900 | 0.010 |
| | 8 | 1 | 1 | 0 | 20 | 1 | 0.096 | 0.009 | 0.911 | 0.911 | 0.009 |
| | 7 | 1 | 1 | 0 | 20 | 1 | 0.084 | 0.008 | 0.922 | 0.922 | 0.008 |
| | 6 | 1 | 1 | 0 | 20 | 1 | 0.071 | 0.007 | 0.933 | 0.933 | 0.007 |
| | 5 | 1 | 1 | 0 | 20 | 1 | 0.059 | 0.006 | 0.944 | 0.944 | 0.006 |
| | 4 | 1 | 1 | 0 | 20 | 1 | 0.047 | 0.005 | 0.955 | 0.955 | 0.005 |
| | 3 | 1 | 1 | 0 | 20 | 1 | 0.035 | 0.003 | 0.967 | 0.967 | 0.003 |
| | 2 | 1 | 1 | 0 | 20 | 1 | 0.023 | 0.002 | 0.978 | 0.978 | 0.002 |
| | 1 | 1 | 1 | 0 | 20 | 1 | 0.012 | 0.001 | 0.989 | 0.989 | 0.001 |
| Normal | 0 | 1 | 1 | 0 | 20 | 1 | 0.000 | 0.000 | 1.000 | 1.000 | 0.000 |
| Overvoltage | -1 | 1 | 1 | 0 | 20 | 1 | -0.011 | -0.001 | 1.011 | 1.011 | -0.001 |
| | -2 | 1 | 1 | 0 | 20 | 1 | -0.023 | -0.002 | 1.022 | 1.022 | -0.002 |
| | -3 | 1 | 1 | 0 | 20 | 1 | -0.034 | -0.003 | 1.033 | 1.033 | -0.003 |
| | -4 | 1 | 1 | 0 | 20 | 1 | -0.045 | -0.004 | 1.044 | 1.044 | -0.004 |
| | -5 | 1 | 1 | 0 | 20 | 1 | -0.056 | -0.005 | 1.055 | 1.055 | -0.005 |
| | -6 | 1 | 1 | 0 | 20 | 1 | -0.067 | -0.006 | 1.066 | 1.066 | -0.006 |
| | -7 | 1 | 1 | 0 | 20 | 1 | -0.078 | -0.007 | 1.077 | 1.077 | -0.007 |
| | -8 | 1 | 1 | 0 | 20 | 1 | -0.089 | -0.008 | 1.088 | 1.088 | -0.008 |
| | -9 | 1 | 1 | 0 | 20 | 1 | -0.100 | -0.009 | 1.099 | 1.099 | -0.009 |
| | -10 | 1 | 1 | 0 | 20 | 1 | -0.110 | -0.011 | 1.111 | 1.100 | 0.000 |

**Table 4-1 : Additional voltage $\Delta V_a$ with $x$ =1**

Initial variation

| | ΔV (pu) % | $S_t$=$S_n$ (pu) | $S_c$ (pu) | $S_{uc}$ (pu) | $S_{sc}$ (pu) | x | $\Delta I_g$ (pu) | $\Delta V_a$ (pu) | $V_{pcc}$(final-Calculated) | $V_{pcc}$(final-Actual) | $\Delta V_a$ (updated) |
|---|---|---|---|---|---|---|---|---|---|---|---|
| Undervoltage | 10 | 1 | 0.5 | 0.5 | 20 | 0.5 | 0.061 | 0.006 | 0.894 | 0.900 | 0.000 |
| | 9 | 1 | 0.5 | 0.5 | 20 | 0.5 | 0.055 | 0.005 | 0.905 | 0.905 | 0.005 |
| | 8 | 1 | 0.5 | 0.5 | 20 | 0.5 | 0.048 | 0.004 | 0.916 | 0.916 | 0.004 |
| | 7 | 1 | 0.5 | 0.5 | 20 | 0.5 | 0.042 | 0.004 | 0.926 | 0.926 | 0.004 |
| | 6 | 1 | 0.5 | 0.5 | 20 | 0.5 | 0.036 | 0.003 | 0.937 | 0.937 | 0.003 |
| | 5 | 1 | 0.5 | 0.5 | 20 | 0.5 | 0.030 | 0.003 | 0.947 | 0.947 | 0.003 |
| | 4 | 1 | 0.5 | 0.5 | 20 | 0.5 | 0.024 | 0.002 | 0.958 | 0.958 | 0.002 |
| | 3 | 1 | 0.5 | 0.5 | 20 | 0.5 | 0.018 | 0.002 | 0.968 | 0.968 | 0.002 |
| | 2 | 1 | 0.5 | 0.5 | 20 | 0.5 | 0.012 | 0.001 | 0.979 | 0.979 | 0.001 |
| | 1 | 1 | 0.5 | 0.5 | 20 | 0.5 | 0.006 | 0.001 | 0.989 | 0.989 | 0.001 |
| Normal | 0 | 1 | 0.5 | 0.5 | 20 | 0.5 | 0.000 | 0.000 | 1.000 | 1.000 | 0.000 |
| Overvoltage | -1 | 1 | 0.5 | 0.5 | 20 | 0.5 | -0.006 | -0.001 | 1.011 | 1.011 | -0.001 |
| | -2 | 1 | 0.5 | 0.5 | 20 | 0.5 | -0.011 | -0.001 | 1.021 | 1.021 | -0.001 |
| | -3 | 1 | 0.5 | 0.5 | 20 | 0.5 | -0.017 | -0.002 | 1.032 | 1.032 | -0.002 |
| | -4 | 1 | 0.5 | 0.5 | 20 | 0.5 | -0.023 | -0.002 | 1.042 | 1.042 | -0.002 |
| | -5 | 1 | 0.5 | 0.5 | 20 | 0.5 | -0.028 | -0.003 | 1.053 | 1.053 | -0.003 |
| | -6 | 1 | 0.5 | 0.5 | 20 | 0.5 | -0.034 | -0.003 | 1.063 | 1.063 | -0.003 |
| | -7 | 1 | 0.5 | 0.5 | 20 | 0.5 | -0.039 | -0.004 | 1.074 | 1.074 | -0.004 |
| | -8 | 1 | 0.5 | 0.5 | 20 | 0.5 | -0.044 | -0.004 | 1.084 | 1.084 | -0.004 |
| | -9 | 1 | 0.5 | 0.5 | 20 | 0.5 | -0.050 | -0.005 | 1.095 | 1.095 | -0.005 |
| | -10 | 1 | 0.5 | 0.5 | 20 | 0.5 | -0.055 | -0.005 | 1.105 | 1.100 | 0.000 |

**Table 4-2 : Additional voltage $\Delta V_a$ with $x$ =0.5**

Initial variation

| | ΔV (pu) % | $S_t=S_n$ (pu) | $S_c$ (pu) | $S_{uc}$ (pu) | $S_{sc}$ (pu) | x | $\Delta I_g$ (pu) | $\Delta V_a$ (pu) | $V_{pcc}$(final-Calculated) | $V_{pcc}$(final-Actual) | $\Delta V_a$ (updated) |
|---|---|---|---|---|---|---|---|---|---|---|---|
| Undervoltage | 10 | 1 | 0 | 1 | 20 | 0 | 0.000 | 0.000 | 0.900 | 0.900 | 0.000 |
| | 9 | 1 | 0 | 0.5 | 20 | 0 | 0.000 | 0.000 | 0.910 | 0.910 | 0.000 |
| | 8 | 1 | 0 | 0.5 | 20 | 0 | 0.000 | 0.000 | 0.920 | 0.920 | 0.000 |
| | 7 | 1 | 0 | 0.5 | 20 | 0 | 0.000 | 0.000 | 0.930 | 0.930 | 0.000 |
| | 6 | 1 | 0 | 0.5 | 20 | 0 | 0.000 | 0.000 | 0.940 | 0.940 | 0.000 |
| | 5 | 1 | 0 | 0.5 | 20 | 0 | 0.000 | 0.000 | 0.950 | 0.950 | 0.000 |
| | 4 | 1 | 0 | 0.5 | 20 | 0 | 0.000 | 0.000 | 0.960 | 0.960 | 0.000 |
| | 3 | 1 | 0 | 0.5 | 20 | 0 | 0.000 | 0.000 | 0.970 | 0.970 | 0.000 |
| | 2 | 1 | 0 | 0.5 | 20 | 0 | 0.000 | 0.000 | 0.980 | 0.980 | 0.000 |
| | 1 | 1 | 0 | 0.5 | 20 | 0 | 0.000 | 0.000 | 0.990 | 0.990 | 0.000 |
| Normal | 0 | 1 | 0 | 0.5 | 20 | 0 | 0.000 | 0.000 | 1.000 | 1.000 | 0.000 |
| Overvoltage | -1 | 1 | 0 | 0.5 | 20 | 0 | 0.000 | 0.000 | 1.010 | 1.010 | 0.000 |
| | -2 | 1 | 0 | 0.5 | 20 | 0 | 0.000 | 0.000 | 1.020 | 1.020 | 0.000 |
| | -3 | 1 | 0 | 0.5 | 20 | 0 | 0.000 | 0.000 | 1.030 | 1.030 | 0.000 |
| | -4 | 1 | 0 | 0.5 | 20 | 0 | 0.000 | 0.000 | 1.040 | 1.040 | 0.000 |
| | -5 | 1 | 0 | 0.5 | 20 | 0 | 0.000 | 0.000 | 1.050 | 1.050 | 0.000 |
| | -6 | 1 | 0 | 0.5 | 20 | 0 | 0.000 | 0.000 | 1.060 | 1.060 | 0.000 |
| | -7 | 1 | 0 | 0.5 | 20 | 0 | 0.000 | 0.000 | 1.070 | 1.070 | 0.000 |
| | -8 | 1 | 0 | 0.5 | 20 | 0 | 0.000 | 0.000 | 1.080 | 1.080 | 0.000 |
| | -9 | 1 | 0 | 0.5 | 20 | 0 | 0.000 | 0.000 | 1.090 | 1.090 | 0.000 |
| | -10 | 1 | 0 | 0.5 | 20 | 0 | 0.000 | 0.000 | 1.100 | 1.100 | 0.000 |

**Table 4-3 : Additional voltage $\Delta V_a$ with $x$ =0**

### 4.3.4 PV Performance during Voltage Disturbances

#### 4.3.4.1AVC contribution

Similar to WTGs, no LVRT or HVRT requirements exist in the ±10% region and accordingly, it can be concluded that *no direct effect* of AVC on PCC-tied PV systems.

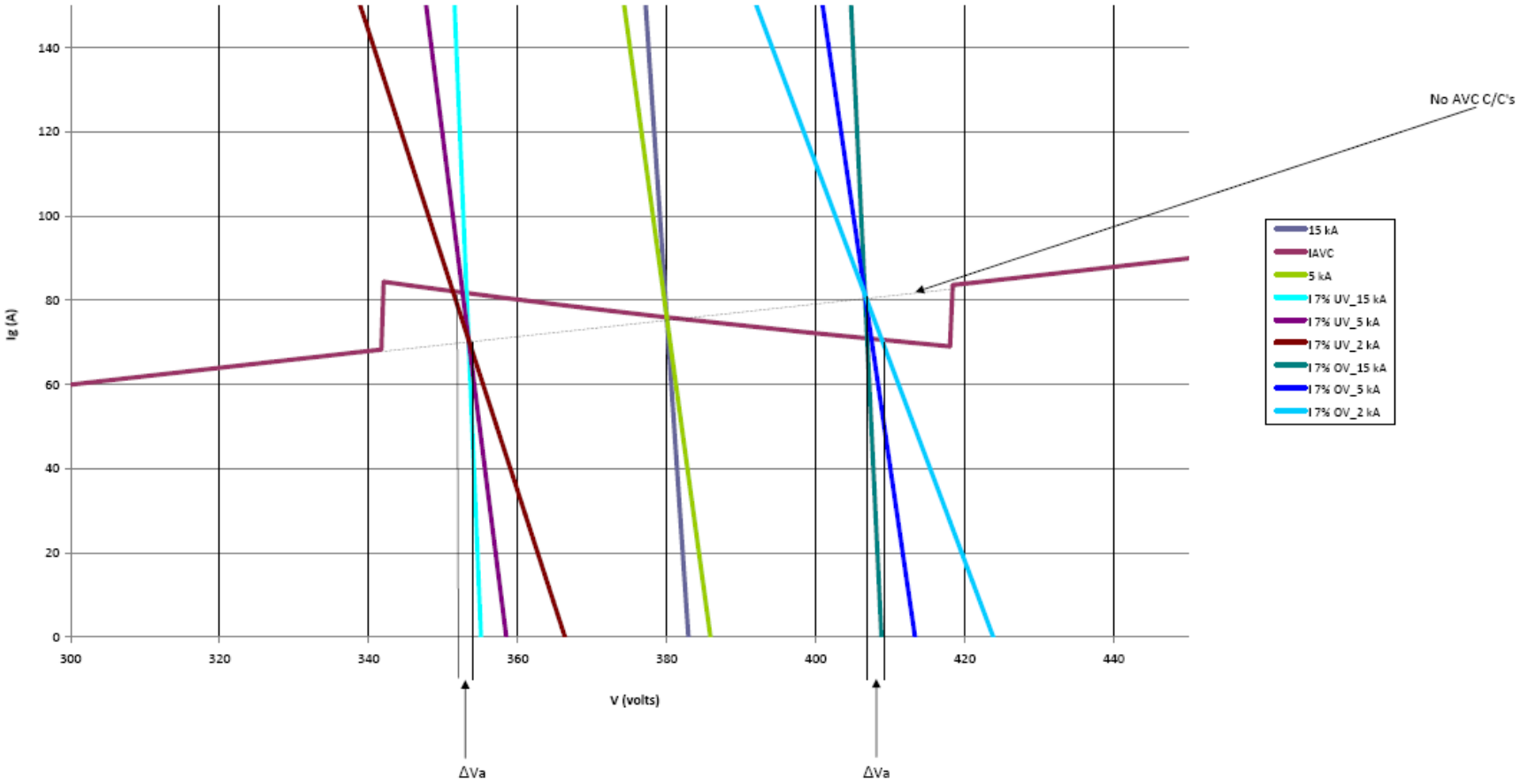


**Figure 4-6 : AVC V-I characteristics vs. system load lines (380 V network example)**

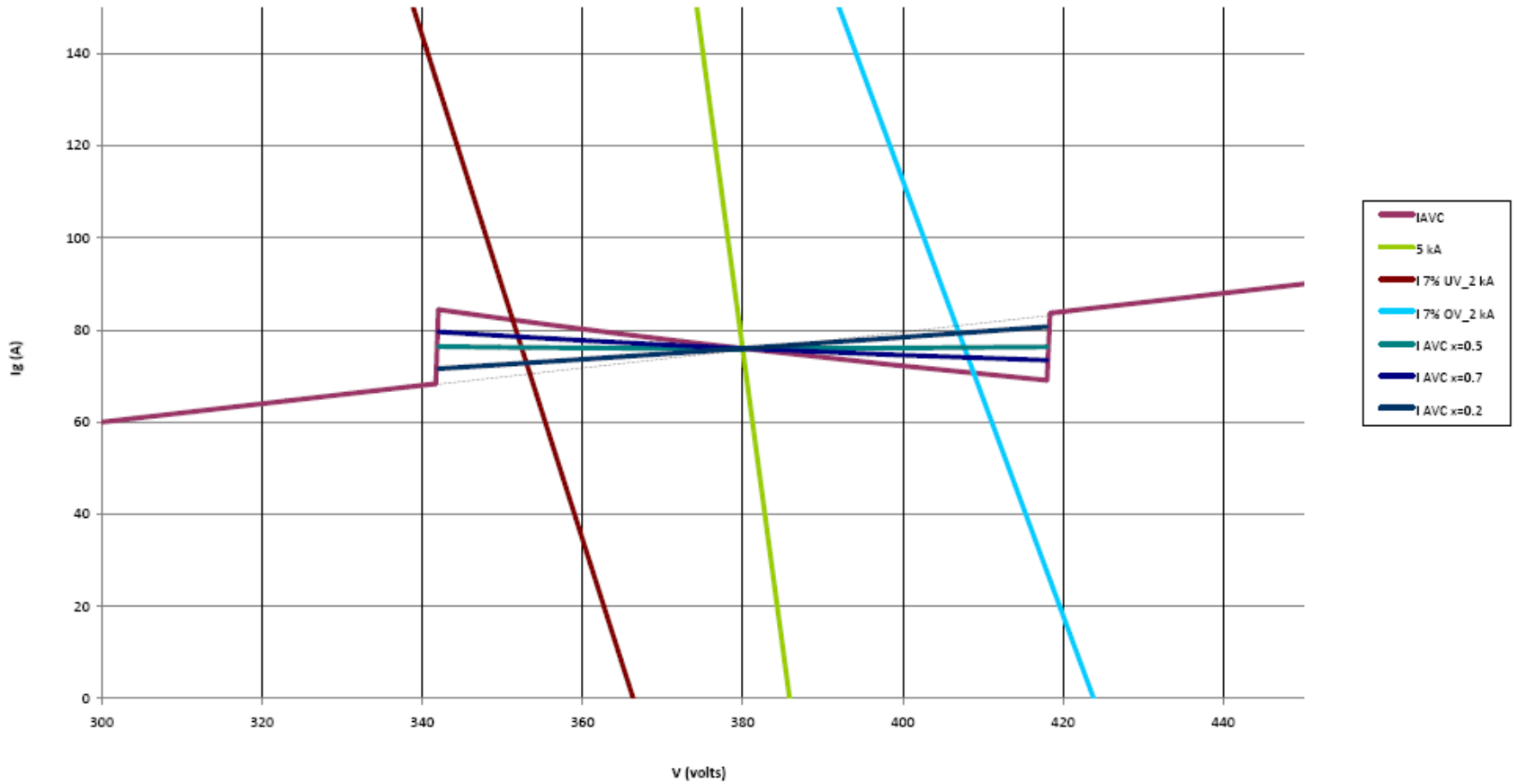


**Figure 4-7 : Variation of conditioning ratio and associated impact (380 V network example).**

# 5 Conclusions and Recommendations

As highlighted in Chapter 1, the study aims to investigate the impact of AVC on modernized grids with renewable energy sources. Modeling the AVC mathematically for grid side interaction had been carried out and equations describing the AVC operation had been derived. Dependency on grid stiffness has been studied and illustrative graphs have been developed. In light of formulated performance model, impact on PCC-tied renewable energy sources has been discussed.

This thesis is an initial attempt to model AVC impact. No papers or research notes on the subject could be located by the time of preparing this thesis.

## 5.1 AVC Technology

The Active Voltage Conditioner (AVC) is very efficient in keeping load voltage constant during system voltage disturbances including dips, swells and voltage flickers. The application areas for AVCs are getting increasingly wide with more sensitive loads being added to industrial networks. AVC is a major addition to Smart Grids with the virtue of controlling load voltage with real-time fluctuations impacting supply voltage and available power due to smart controllers.

The AVC transforms the connected load from constant impedance load to constant active and reactive power load within operational conditioning range (±10% typically).

It impacts the voltage at Point of Common Coupling (PCC) by increasing the voltage dips and swells magnitudes. Due to AVC operation and inverse gradient V-I characteristics, PCC undervoltages are more susceptible to get deeper than equal-in-magnitude overvoltages.

## 5.2 Impact on Grid with Renewable Energy Sources

The AVC impact on grid performance can be explained by the additional demand during voltage variations and resulting additional voltage drop/rise on Point of Common Coupling (PCC). Nevertheless; the study demonstrates that the operation of AVCs *does not cause* additional voltages to exceed the ±10%. Most utilities have no LVRT or HVRT

requirements in this voltage region and accordingly, it is envisaged that integrating AVCs does not impact LVRT or HVRT directly.

Additional drop/rise depends on the conditioning ratio on the PCC (loads connected through AVCs) and system available short circuit current. Values up to 2% can occur with weak/remote LV/MV networks where it is common to get a renewable distributed power generation source tied.

In the case of the operational range of AVC is extended beyond the ±10%, the additional demand and voltage drop will increase the reactive power support requirement for LVRT and HVRT.

## 5.3 Further Research

There is a wide future area of studies on AVCs due to the lack of detailed investigation on grids with high renewable energy penetration, including the impact of AVCs on:

- Frequency stability
- Rotor angle stability
- System performance during wind/PV power loss
- Voltage collapse
- Reverse power flow (AVC upstream)
- Harmonic currents
- Ride-through requirements if AVC operational range is extended beyond ±10%
- Dynamic short time compensation
- Grid stability in case of system islanding

Advanced network simulations with IEEE-9 and IEEE-30 buses system models will be needed to carry out further stability investigations. AVCs may be incorporated in a small scale grid/smart grid test-bed with non-linear loads to verify the system performance during disturbances in presence of harmonics.

By examining the AVC derived model, if the AVC operational range is extended beyond ±10% for specific needs and where the conditioned load is seemingly reasonable compared with grid capacity, ride-through capability of coupled wind farms and solar PV

systems may need to be revised to allow for additional reactive power requirement. Detailed computer simulation will be required to verify the additional requirement taking into consideration the impact of Constant Power Load (CPL) on system stability.

Another subject for research exists for remedial solutions to keep AVC running without impacting PCC voltages. Depending on the "severity" of the additional PCC voltage variations, a detailed cost-benefit analysis may be carried out to justify adding battery banks connected to AVC DC bus in order to compensate the additional/subtractive demand. AVC physical design may be affected with energy storage elements.

Impact on islanded systems may be investigated with an eye on the accelerated voltage collapse scenario that can take place during renewable power input fluctuations (e.g. wind speed, shadow on PV cells…etc).

# References and Bibliography

[1] Global Wind Energy Council: www.gwec.net

[2] Hand, M.M.; Baldwin, S.; DeMeo, E.; Reilly, J.M.; Mai, T.; Arent, D.; Porro, G.; Meshek, M.; Sandor, D. eds.," Renewable Electricity Futures Study," *4 Vols. NREL/TP-6A20-52409. Golden, CO: National Renewable Energy Laboratory, 2012.* http://www.nrel.gov/analysis/re_futures/.

[3] J Keir and Simon Walton,"Cost Effective Active Voltage Conditioning," *Australian Journal of Electrical & Electronics Engineering, Vol. 1, No.2, 2004.*

[4] EN 50160, "Voltage characteristics of electricity supplied by public distribution networks," 2007.

[5] M Brenna, E De Berardinis, L D Carpini, F Foiadelli, P Paulon, P Petroni, G Sapienza, G Scrosati and Dario Zaninelli," Automatic Distributed Voltage Control Algorithm in Smart Grids Applications," *IEEE Transactions On Smart Grid, Vol. 4, No. 2, June 2013, pp.877-885.*

[6] Vijay Vittal and Raja Ayyanar, "Grid Integration and Dynamic Impact of Wind Energy," *doi: 10.1007/978-1-4419-9323-6, Springer Science+Business Media, New York, 2013.*

[7] S Engelhardt, I Erlich, C Feltes, J Kretschmann and F Shewarega, "Reactive Power Capability of Wind Turbines Based on Doubly Fed Induction Generators," *IEEE Transactions on Energy Conversion, Vol. 26, No. 1, March 2011, pp.364-372.*

[8] Z Chen, J M. Guerrero and F Blaabjerg," A Review of the State of the Art of Power Electronics for Wind Turbines," *IEEE Transactions on Power Electronics, Vol. 24, No. 8, August 2009, pp.1859-1875.*

[9] S. M. Muyeen, A. Al-Durra and H. M. Hasanien, "Modeling and Control Aspects of Wind Power Systems," *DOI: 10.5772/3405, InTech, 2013.*

[10] T. Orłowska-Kowalska et al. (eds.)," Advanced and intelligent control in power electronics and drives," *Studies in Computational Intelligence 531, doi: 10.1007/978-3-319-03401-0_2, Springer International Publishing Switzerland, 2014.*

[11] Md. Emdadul Haque, S. Paul, and Md. R. I. Sheikh, "Grid Frequency Analysis with the Issue of High Wind Power Penetration," in *International Conference on Electrical Information and Communication Technology (EICT), 2013*.

[12] Eknath Vittal, Mark O'Malley and Andrew Keane," Rotor Angle Stability With High Penetrations of Wind Generation"*, IEEE Transactions on Power Systems, Vol. 27, No. 1, February 2012, pp.352-362.*

[13] J Merino, C Veganzones, Jose A. Sanchez, S Martinez and Carlos A. Platero, "Power System Stability of a Small Sized Isolated Network Supplied by a Combined Wind-Pumped Storage Generation System: A Case Study in the Canary Islands," *Energies 2012, 5, 2351-2369; doi:10.3390/en5072351.*

[14] M. J. Hossain, T. K. Saha and N. Mithulananthan," Impacts of wind and solar integrations on the dynamic operations of distribution systems," *The school of ITEE, The University of Queensland, St.Lucia, Brisbane, QLD-4072, Australia.*

[15] P G. Barbosa, Luís G.B. Rolim, Vladimir V. Tavare, Edson H. Watanabe and R. Hanitsch, "Novel Control Strategy for Grid-Connected DC-AC Converters with Load Power Factor and MPPT Control," http://www.solar.coppe.ufrj.br/rolim.html

[16] IEEE Std. 929-2000, "IEEE Recommended Practice for Utility Interface of Photovoltaic (PV) Systems,"

[17] Ewald F.Fuchs and Mohammed A.S. Masoum, "Power Quality in Power Systems and Electrical Machines," *Academic Press; 1st edition (March 7, 2008).*

[18] IEEE Std. 1159-1995, "Recommended Practice on Monitoring Electric Power Quality,"

[19] Rolf Grünbaum, "Voltage and Power Quality Control in Wind Power Applications by Means of Dynamic Compensation," *ABB Power System AB, Sweden*.

[20] G Xiao, Z Zeng , K Liu , Z Hu and Zhaoan Wang, "Novel Active Voltage Quality Regulator with Adaptive DC-Link Voltage Control," *Journal of Power Electronics, Vol. 11, No. 6, November 2011.*

[21] Yong Lu, G Xiao, Bo Lei, X Wu and S Zhu," A Transformerless Active Voltage Quality Regulator With the Parasitic Boost Circuit," *IEEE Transactions on Power Electronics, Vol. 29, No. 4, April 2014, pp. 1746- 1756.*

[22] Guochun Xiao & others," Phase shift control for series active voltage quality regulator," *Journal of Power Electronics, Vol. 12, No. 4, July 2012.*

[23] ABB, "Case Study - PCS100 Active Voltage Regulator (AVR)," http://www05.abb.com/global/scot/scot232.nsf/veritydisplay/8cb3000da66fdcaf48257920006e4efe/$file/2UCD301118_a%20PCS100%20AVR%20Case%20Study%20-%20English%20vers.pdf

[24] www.plexim.com.

[25] Mónica Alonso and Hortensia Amarís, "Impact of Wind Farms in Power Networks, Wind Farm - Impact in Power System and Alternatives to Improve the Integration," *Dr. Gastón Orlando Suvire (Ed.), InTech, 2011.*

[26] M Molinas, D Moltoni, G Fascendini, J A Suul and T Undeland, "Constant Power Loads in AC Distribution Systems: an investigation of stability," *IEEE International Symposium on Industrial Electronics, ISIE 2008, Cambridge, June 30-July 2, pp.1531 – 1536.*

[27] E. Morales, "Voltage Regulation and Reactive Power Support via Photovoltaic Inverters as a Smart Grid Application," M.Sc Thesis, *The University of Texas at San Antonio, College of Engineering, Department of Electrical and Computer Engineering December 2011.*

[28] Almoataz Y. A, Amr M. Ibrahim, Ahmed M. Asim, Ahmed H. Abdel Razek, "Dynamic Behaviour of DFIG-Based Wind Turbines During Symmetrical Voltage Dips," *Electrical and Electronics Engineering: An International Journal (ELELIJ) Vol. 2, No 2, May 2013.*

[29] B. Renders, K. De Gussemé, L. Degroote, B. Meersman and L. Vandevelde, "Voltage Dip Ride-Through Capability of Converter-Connected Generators," *International Conference on Renewable Eenergies and Power Quality (ICREPQ), 2007.* http://www.icrepq.com/icrepq07/287-renders.pdf

[30] J. Tian, C. Su and Z. Chen," Reactive Power Capability of the Wind Turbine with Doubly Fed Induction Generator," *Industrial Electronics Society, IECON 2013 - 39th Annual Conference of the IEEE , Vienna, 10-13 Nov. 2013,pp. 5312 – 5317.*

[31] S. Mishra, S. Shukla and Shimi.S.L," Performance Analysis and Limitations of Grid Connected DFIG Wind Turbine under Voltage Sag and 3-Phase Fault," *International Journal of Engineering Research and Development, e-ISSN: 2278-067X, p-ISSN: 2278-800X, www.ijerd.com, Vol. 10, Issue 8 (August 2014), PP.51-62.*

[32] X. Zhang, X. Cao, W. Wang and C. Yun," Fault Ride-Through Study of Wind Turbines," *Journal of Power and Energy Engineering, 2013, 1, 25-29 http://dx.doi.org/10.4236/jpee.2013.15004, Published Online October 2013 (http://www.scirp.org/journal/jpee)*

[33] Aparicio, N., Chen, Z., Beltran, H., & Belenguer, E., "Performance of Doubly-Fed Wind Power Generators During Voltage Dips," *Paper presented at International Workshop on Next Generation Regional Energy System Development, IWRES07, Seoul,* 2007.

[34] J Sun, "Impedance-Based Stability Criterion for Grid-Connected Inverters," *IEEE Transactions on Power Electronics, Vol. 26, No.11, November 2011, pp. 3075-3078.*

[35] Anne Labouret and Michel Villoz, "Solar Photovoltaic Energy," *IET Renewable Energy Series 9, The Institution of Engineering and Technology, www.theiet.org , 2010.*

[36] K Perutka, "MATLAB For Engineers – Applications in Control, Electrical Engineering, IT and Robotics," *InTech, 2011.*

[37] Ali Keyhani, M. N. Marwali and Min Dai, "Integration of Green and Renewable Energy in Electric Power Systems," *John Wiley & Sons, 2010.*

[38] https://products.office.com/en-us/visio/flowchart-software

[39] F. Mekri, M. Machmoum, N. Aït-Ahmed and B. Mazari, "A comparative study of voltage controllers for series active power filter," *Electric power systems research 80 (2010) 615-626.*

[40] R. Shah, N. Mithulananathan, R. Bansal, K. Y. Lee and A. Lomi, "Influence of Large-scale PV on Voltage Stability of Sub-transmission System," *International Journal on Electrical Engineering and Informatics, Vol. 4, number 1, March 2012.*

[41] A. B. Mayilvaganan, S. S. Dash and V. Venkataramanan, "Grid Voltage Stability Enhancement Using Photovoltaic Based Static Synchronous Compensator," *Journal of Computer Science, 9 (3): 299-307, 2013.*

[42] M. García-Gracia, M. Paz Comech,J. Sallán, A. Llombart, "Modeling wind farms for grid disturbance studies," *Renewable Energy 33 (2008) 2109–2121.*

[43] Sang-Jin Kim and Se-Jin Seong, "A Simple Prediction Model for PCC Voltage Variation Due to Active Power Fluctuation for a Grid Connected Wind Turbine, Wind Turbines," *Dr. Ibrahim Al-Bahadly (Ed.), ISBN: 978-953-307-221-0, InTech, 2011.*

[44] Jeju Island Smart Grid Test-Bed, South Korea http://www.smartgrid.or.kr/10eng3-1.php

[45] William D. Stevenson, Jr. "Elements of Power System Analysis," *McGraw Hill Higher Education; 4th edition (1982).*

[46] P. Kundur,"Power System Stability and Control," *McGraw Hill Professional Publishing; 1st edition (1994).*

[47] Dr. Eng. Mohamed EL-Shimy; Lectures online http://shimymb.tripod.com